

Image Reconstruction in Optical Long-Baseline Interferometry

Karl-Heinz Hofmann, Max-Planck-Institut for Radioastronomy Bonn

VLTI winter school, Garching, March 6-8 2017

Outline:

- Why model independent imaging?
- Observed interferometric data
- Reconstruction constraints based on the measured data
- Regularization
- Minimization algorithms to find the reconstructed image
- IRBis
- Enough data for image reconstruction?
- Image reconstruction session with IRBis
- Outlook

Why model-independent imaging?

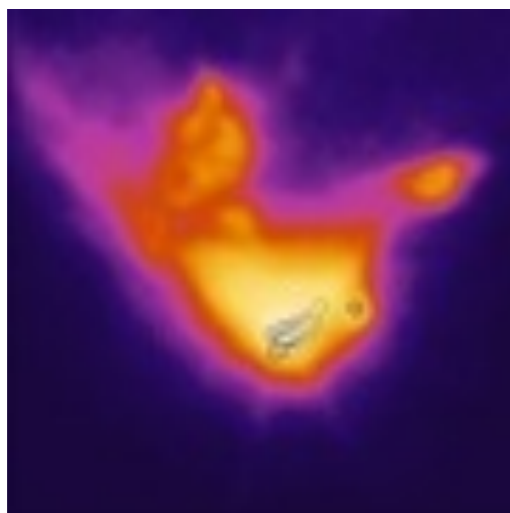
For targets with too complex structure, model fitting not useful

- a model with wrong geometry can fit well, even with moderate uv coverage
- the best-fit parameters are completely meaningless.

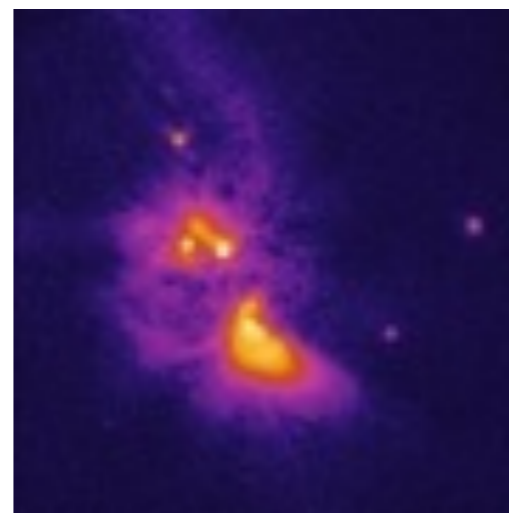
Imaging is often the only way to get insight in complex structures.

Images can be interpreted and analysed straight-forwardly by colleagues who are not familiar with interferometry.

With images your results are better presented and improve funding prospects.



R Mon



Mon R2

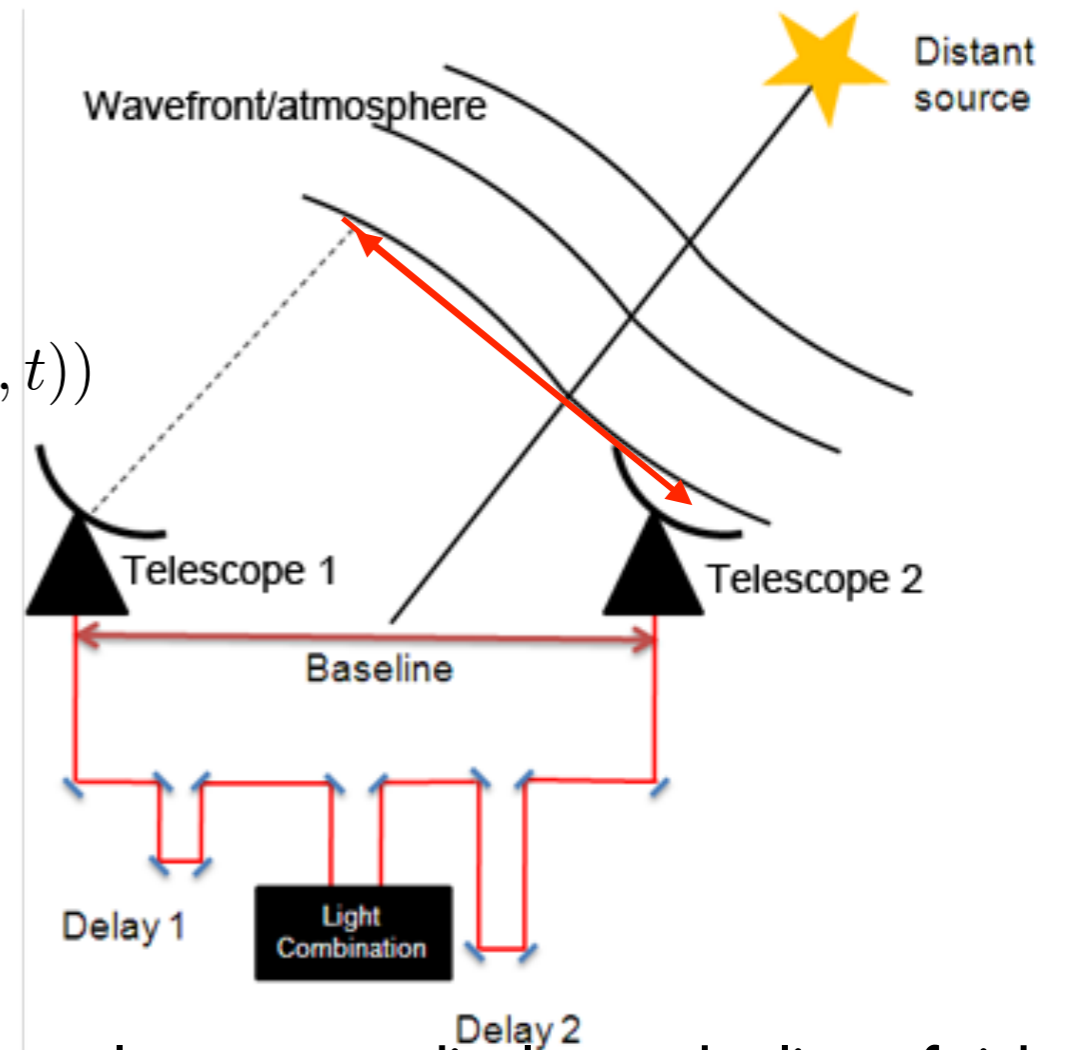
*Bispectrum speckle
interferometry obs.
of young stellar objects
with diffraction-limited
resolution*

Observed interferometric data

Output of an interferometer:

each baseline provides one complex visibility

$$I(f_{12}(t)) = O_\lambda(f_{12}(t)) \cdot \exp(i\phi_1(\lambda, t)) \cdot \exp(-i\phi_2(\lambda, t))$$



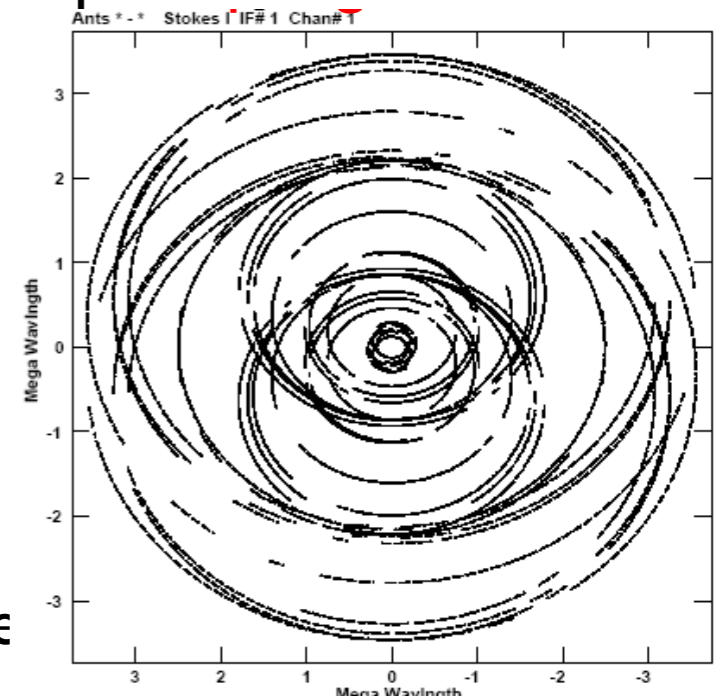
- projected baseline: $b_{ij}(t) = r_j(t) - r_i(t)$
 $r_i(t)$ = position of the i-th telescope projected on a plane perpendicular to the line of sight
- $f_{ij}(t) = b_{ij}(t)/\lambda$: spatial frequency
- $O_\lambda(f_{ij}(t))$ = angular Fourier transform of the observed object $O_\lambda(\alpha)$ in angular direction α
- $\phi_i(\lambda, t)$ = atmospherically distorted phase of the incoming wavefront and instrumental phase at telescope i
- λ = wavelength
- t = time

Special case: Image reconstruction = deconvolution

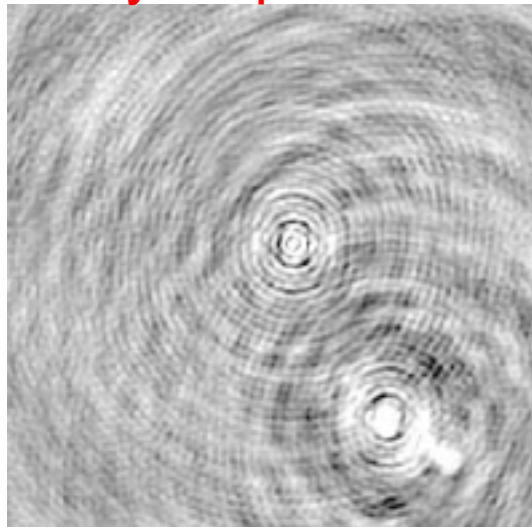
- All measured complex visibilities $O(f_{ij})$ cover a small fraction of the uv plane
- Use all measured complex visibilities to reconstruct an image: this is a simple Fourier inversion

$$i(x) = \int_{f_{ij} \in M} O(f_{ij}) \exp(2\pi i f_{ij} \mathbf{x}) df_{ij}$$

the „dirty map“ $i(x) = o(x) \otimes p(x)$ is true object $o(x)$ convolved with the „dirty beam“ $p(x)$ caused by the sparse uv coverage

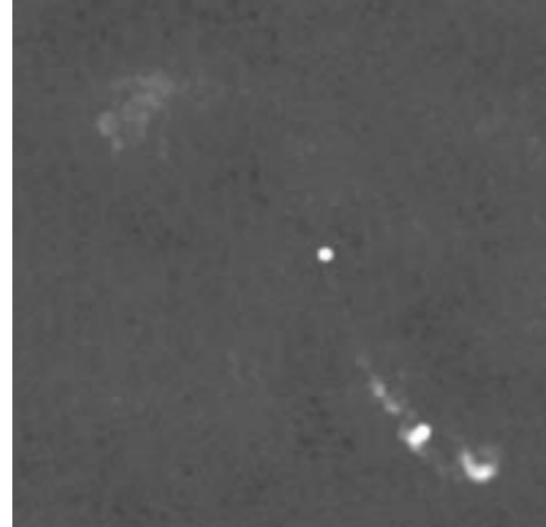


dirty map



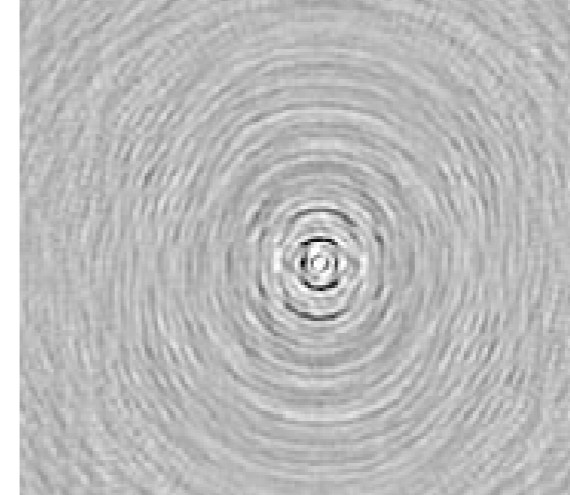
=

true object



*

dirty beam



Simon Garrington

Radio
interferometry
example

the image looks bad because of the sparse uv coverage.
prior information about the object has to be applied to get correct images.

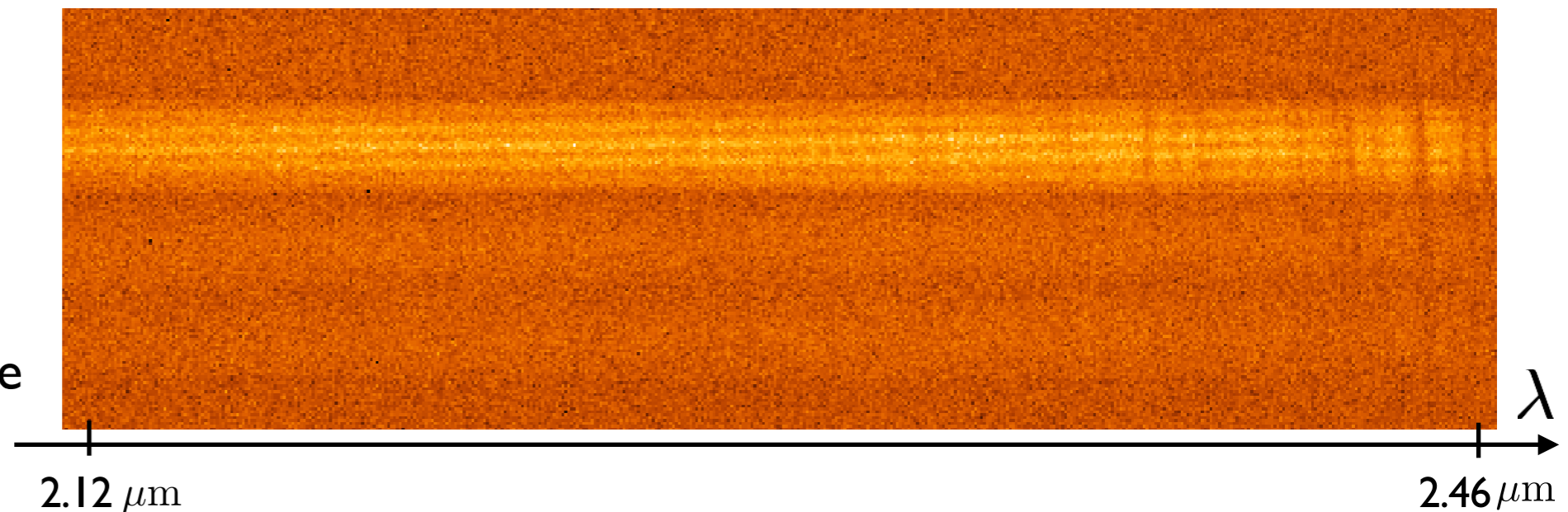
BUT, usually, we have no complex visibilities in optical long baseline interferometry !!

Effects of the turbulent atmosphere:

- Due to the **fast turbulent atmosphere**, IR interferograms have to be recorded with **short exposure times** of $\sim 10 - 300$ ms in order to „freeze the interferometric fringes“ containing the high-spatial frequency information, i.e. the object Fourier transform $O_\lambda(f_{ij}(t))$. The **exposure time is similar to** the time-interval in which the atmosphere stays constant, the so called **coherence time**.
- The **interferograms are degraded** by photon- and detector-noise

VLT/AMBER:

- interferogram
- ~ 1 spectral channel per pixel column
- fringes visible
- detector noise visible
- IRAS 13481, $K =$



- **Fringe contrast is the visibility** $|O_\lambda(f_{ij}(t))|$ of the Fourier transform $O_\lambda(f_{ij}(t))$ of the target
- **Fringe phase is the Fourier phase** of $O_\lambda(f_{ij}(t))$ plus the unknown atmospheric phase

Effects of the turbulent atmosphere:

- power spectrum

$$\langle |I(f_{12})|^2 \rangle_m = |O_\lambda(f_{12})|^2 \cdot \langle |\exp(i\phi_1(\lambda, t)) \cdot \exp(-i\phi_2(\lambda, t))|^2 \rangle_m > 0$$

power spectrum is not sensitive to phase errors!

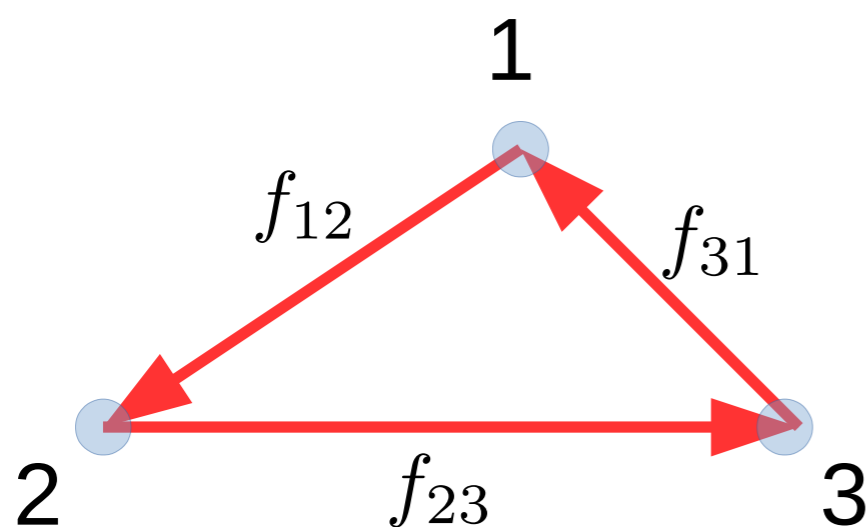
- bispectrum

$$\begin{aligned} \langle I(f_{12}) I(f_{23}) I(f_{31}) \rangle_m &= O_\lambda(f_{12}) O_\lambda(f_{23}) O_\lambda(f_{31}) \times \\ &\times \langle \exp(i[\phi_1(\lambda, t) - \phi_2(\lambda, t) + \phi_2(\lambda, t) - \phi_3(\lambda, t) + \phi_3(\lambda, t) - \phi_1(\lambda, t)]) \rangle_m > 0 \end{aligned}$$

bispectrum is not sensitive to phase errors!

with $f_{12} + f_{23} + f_{31} = 0 \longrightarrow O_\lambda(f_{12}) O_\lambda(f_{23}) O_\lambda(f_{31}) = O_\lambda(f_{12}) O_\lambda(f_{23}) O_\lambda(-f_{12} - f_{23})$
 $= O_\lambda(f_{12}) O_\lambda(f_{23}) O_\lambda^*(f_{12} + f_{23})$
 $=: O_\lambda^{(3)}(f_{12}, f_{23})$

„Closing Triangle“



for real objects: $O_\lambda(-f_{12}) = O_\lambda^*(f_{12}) = O_\lambda(f_{21})$
 $\Phi_{21} = -\Phi_{12}$

Closure Phase $\Phi_{123} := \Phi_{12} + \Phi_{23} + \Phi_{31}$
 = sum of the object Fourier phases

$$O_\lambda(f_{12}) := V_{12} \cdot \exp(i\Phi_{12})$$

Effects of the turbulent atmosphere:

BUT in special cases

- complex visibilities

can be measured in optical/infrared interferometry:

- a) beam combiners providing spectral information like AMBER, GRAVITY & MATISSE are able to measure **wavelength-differential phases**; wavelength-differential phases are obtained after rough compensation of the atmospheric phases;
from wave-length differential phases the absolute Fourier phases and complex visibility can be derived
(as proposed by Millour and Petrov).
- b) GRAVITY also measures **complex visibilities through phase-referencing** (a close by star is used to determine the atmospheric phases of the target which are compensated before averaging the interferograms).

Properties of the interferometric data:

- non-linear data

power spectrum $\sim |I(f)|^2$

bispectrum $\sim I(f_1) I(f_2) I^*(f_1 + f_2)$

- linear data

complex visibilities

- sparsity of the uv coverage of the data

holes in the uv plane
 (typical for present optical/IR
 interferometers due small number
 of telescopes, $\sim 3-6$)

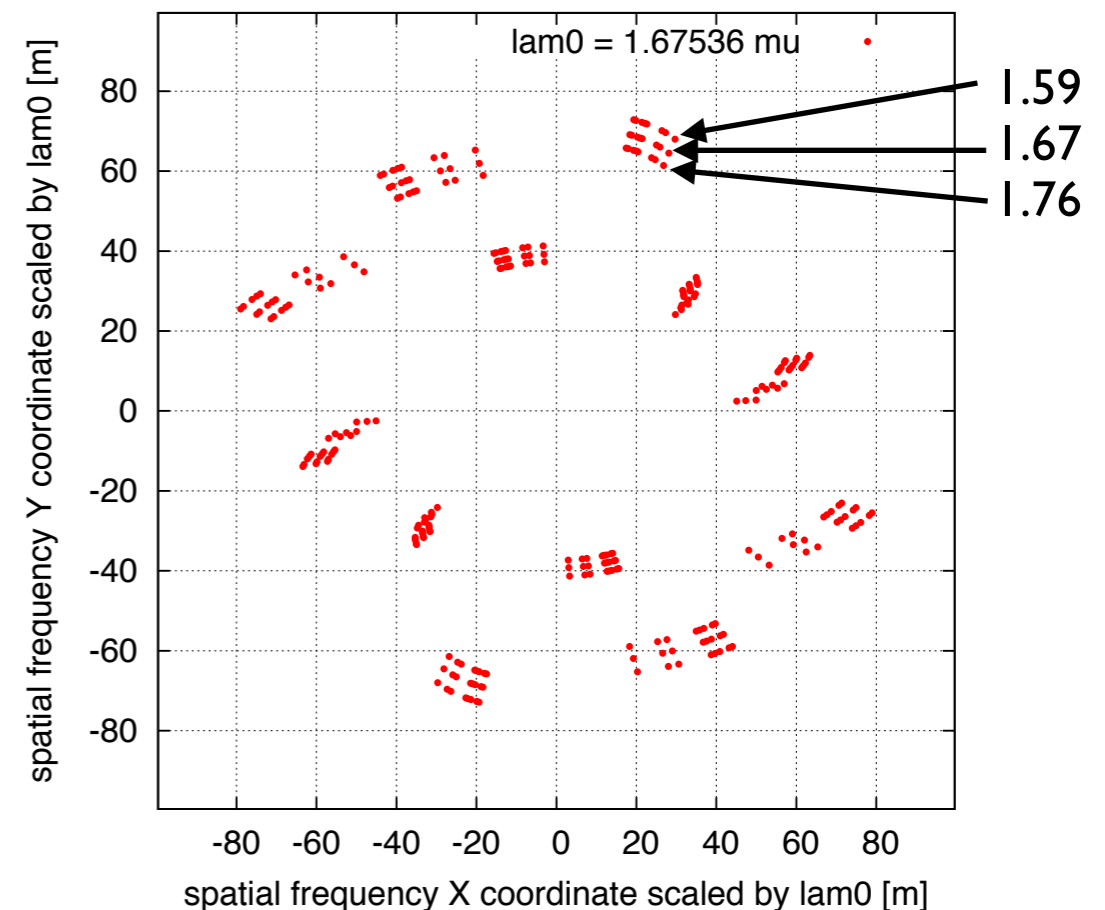
- Fourier phase information

power spectrum : has no Fourier phase

bispectrum : provides a sum of 3 Fourier phases, no single Fourier phases

complex visibilities: all Fourier phases

spatial frequency plane



Input data

- Squared visibilities (power spectra) and the closure phases (phase of the complex bispectrum)
- Some algorithms, e.g. IRBis, use the bispectrum $O^{(3)}(\mathbf{f}_u, \mathbf{f}_v)$ built by the measured

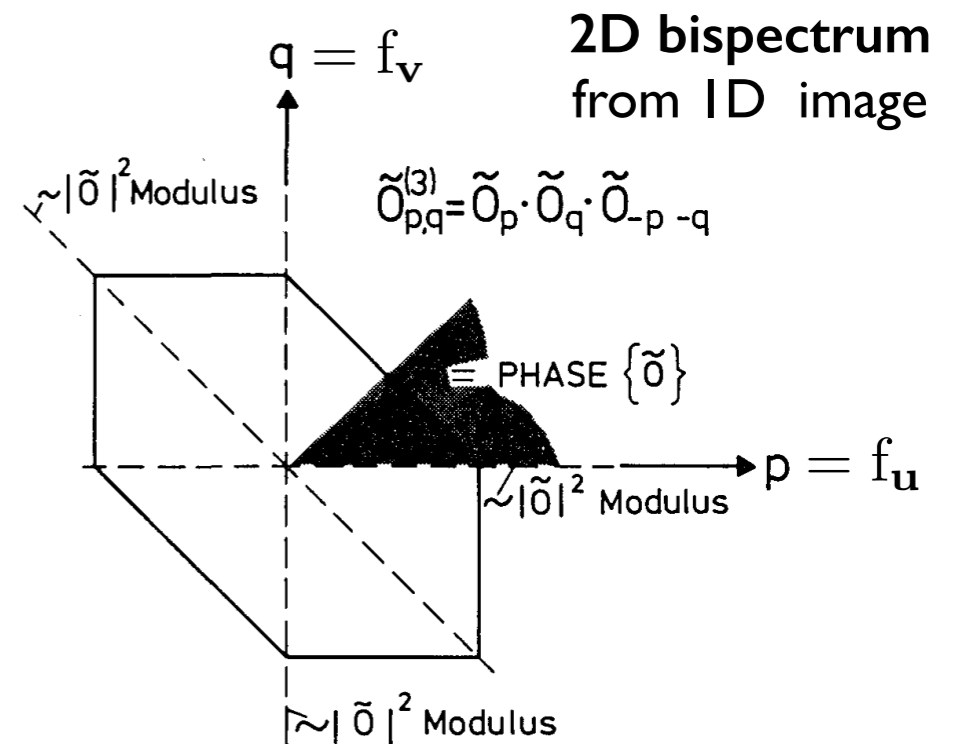
squared visibilities $V^2(\mathbf{f}_u)$ and the measured closure phases $\beta(\mathbf{f}_u, \mathbf{f}_v)$:

$$O^{(3)}(\mathbf{f}_u, \mathbf{f}_v) = O(\mathbf{f}_u) O(\mathbf{f}_v) O^*(\mathbf{f}_u + \mathbf{f}_v)$$

$$= \sqrt{V^2(\mathbf{f}_u) V^2(\mathbf{f}_v) V^2(\mathbf{f}_u + \mathbf{f}_v)} \exp \{i \beta(\mathbf{f}_u, \mathbf{f}_v)\}$$

- bispectrum also contains the squared visibilities $V^2(\mathbf{f}_u)$ on the three axis in the bispectrum plane, e.g. if $\mathbf{f}_v = 0$

- bispectrum of 2-dimensional image is 4-dimensional



- the error of the bispectrum built is calculated from the errors of $V^2(\mathbf{f}_u)$ and $\beta(\mathbf{f}_u, \mathbf{f}_v)$
- this bispectrum is not complete because of the sparsity of the uv coverage.

Constraints due to the measured data

- The **bispectrum (including the power spectrum)** is a good observable in **optical/IR interferometry** — the bispectrum is insensitive to phase errors due to the atmosphere and the interferometry instrument.
- The **complex visibility** is in special cases also a good observable in **optical/IR interferometry**:
 - a) when wavelength-differential phases can be measured (AMBER/GRAVITY/MATISSE)
 - b) with phase referencing (GRAVITY)
- The task of each image reconstruction in optical/IR interferometry is „to find that image which is consistent with the bispectrum data or complex visibility data“

IRBis is able to handle bispectrum and complex visibility data

I will discuss the imaging with bispectrum data only

Constraints due to the measured data

- Since measured bispectrum is an average over many frames the errors obey Gaussian statistics: the consistency of the image with measured bispectrum can be estimated by χ^2 statistics

$$\chi^2 = \frac{1}{N} \int_{(\mathbf{f}_u, \mathbf{f}_v) \in M} \left| \frac{O_k^{(3)}(\mathbf{f}_u, \mathbf{f}_v) - O^{(3)}(\mathbf{f}_u, \mathbf{f}_v)}{\sigma(\mathbf{f}_u, \mathbf{f}_v)} \right|^2 d\mathbf{f}_u d\mathbf{f}_v \approx 1$$

bispectrum of the image
bispectrum errors
measured bispectrum

if $\chi^2 \approx 1$ (N = number of measured bispectrum elements):

\longrightarrow the difference between the measured bispectrum and the bispectrum of the reconstructed image is about the bispectrum error \longrightarrow
 the image is consistent with the measured bispectrum

- This **direct fit to the bispectrum** is used in nearly all present image reconstruction algorithms.

This **direct fit to the bispectrum** for image reconstruction was first proposed in the Building Block Method (BBM) by Hofmann & Weigelt 1991, 1993.

Constraints due to the measured data

The IRBis algorithm, an extension of the BBM, uses the following χ^2 function:

$$Q[o_k(\mathbf{x})] := \int_{\mathbf{f}_u, \mathbf{f}_v \in M} \frac{w_d(\mathbf{f}_u, \mathbf{f}_v)}{\sigma^2(\mathbf{f}_u, \mathbf{f}_v)} \cdot |\gamma_0 O_k^{(3)}(\mathbf{f}_u, \mathbf{f}_v) - \underbrace{O^{(3)}(\mathbf{f}_u, \mathbf{f}_v)}_{\text{measured bispectrum}}|^2 d\mathbf{f}_u d\mathbf{f}_v$$

- $o_k(\mathbf{x})$: actual iterated image, and \mathbf{x} is a 2D image space vector
- $O_k^{(3)}(\mathbf{f}_u, \mathbf{f}_v)$: bispectrum of the iterated image
- $w_d(\mathbf{f}_u, \mathbf{f}_v)$: weight to compensate for the unequal distribution of the uv points
(it is proportional to the inverse of the uv point density)
- $\sigma(\mathbf{f}_u, \mathbf{f}_v)$: errors of the measured bispectrum
- γ_0 : scaling factor to minimize the value of Q during each iteration step,
i.e. $o_k(\mathbf{x})$ will be not normalised to integral = 1;
- $\mathbf{f}_u, \mathbf{f}_v \in M$: the amount of all measured bispectrum elements

$Q[o_k(\mathbf{x})]$ is also called the „data penalty term“ or „likelihood term“

Regularization

Because of the **sparse uv coverage**, the **noise in the data** and the **non-linearity of the data**

➔ many local minima of the χ^2 function exist, and therefore many solutions does exist which could fit the data within the error bars

➔ the algorithm has to be helped to find the right solution by introducing **prior information about the target**:

- **prior info is to force positivity** of the reconstruction — all observed astronomical targets are intensity distributions ➔ have positive values; this is introduced by the minimization routine as discussed later.
- **prior info is the knowledge about the extent of the target**: the restriction of the reconstruction area avoids spikes in the Fourier plane between the observed uv points: small structures ➔ smooth Fourier transform.
the reconstruction region can be realised by a) restricting the FOV to be reconstructed and b) by an binary mask in image space (IRBis)
- **prior info is also, for example, smoothness of the target**: most targets don't have a „noisy structure“ but mostly a smooth one

Regularization

- prior info is introduced by adding a weighted regularization term $H[o_k(\mathbf{x})]$ to the data constraint term $Q[o_k(\mathbf{x})]$
- the algorithm tries to minimize the cost function

$$J[o_k(\mathbf{x})] := Q[o_k(\mathbf{x})] + \mu \cdot H[o_k(\mathbf{x})] \quad (\text{cost function})$$

μ : regularization parameter defining the strength of the influence of $H[o_k(\mathbf{x})]$

- this kind of cost function contain nearly all (or all) image reconstruction algorithms in optical interferometry

- the goal of the regularization functions is to select that image $o_k(\mathbf{x})$

out of the pool of all images with $\chi^2 \approx 1$ (many could exist because of sparse uv coverage) which has value of $H[o_k(\mathbf{x})]$ that is closest to the minimum of H

Regularization - regularization functions

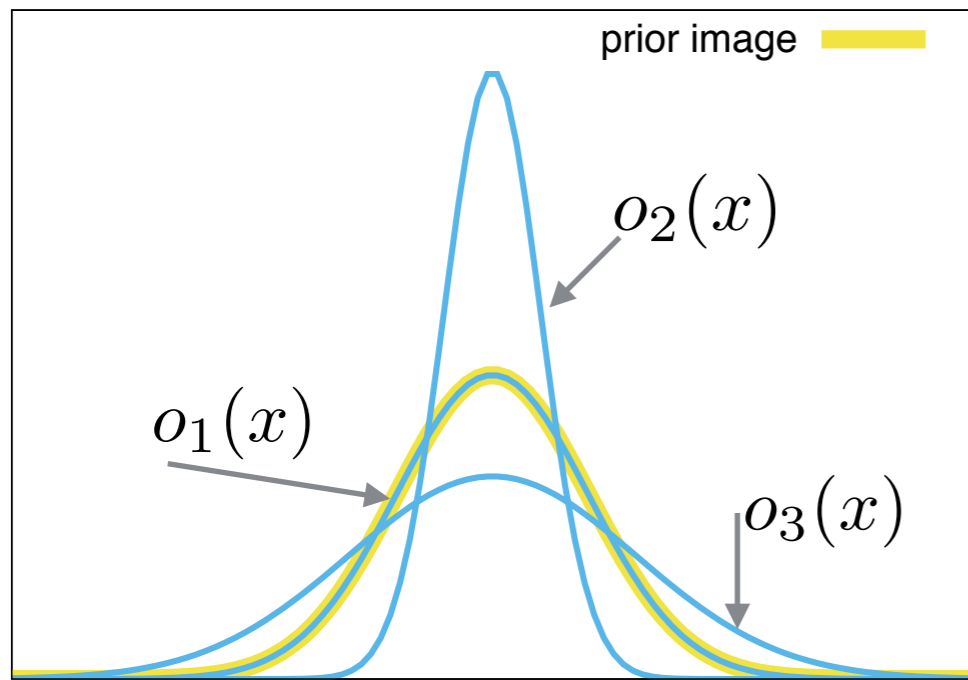
1. „Pixel intensity“ quadratic regularization enforcing smoothness

$$H[o_k(\mathbf{x})] := \int \frac{o_k(\mathbf{x})^2}{prior(\mathbf{x})} d\mathbf{x}$$

prior(x): can be a) an estimate of the target,
or b) a constant, if target size unknown

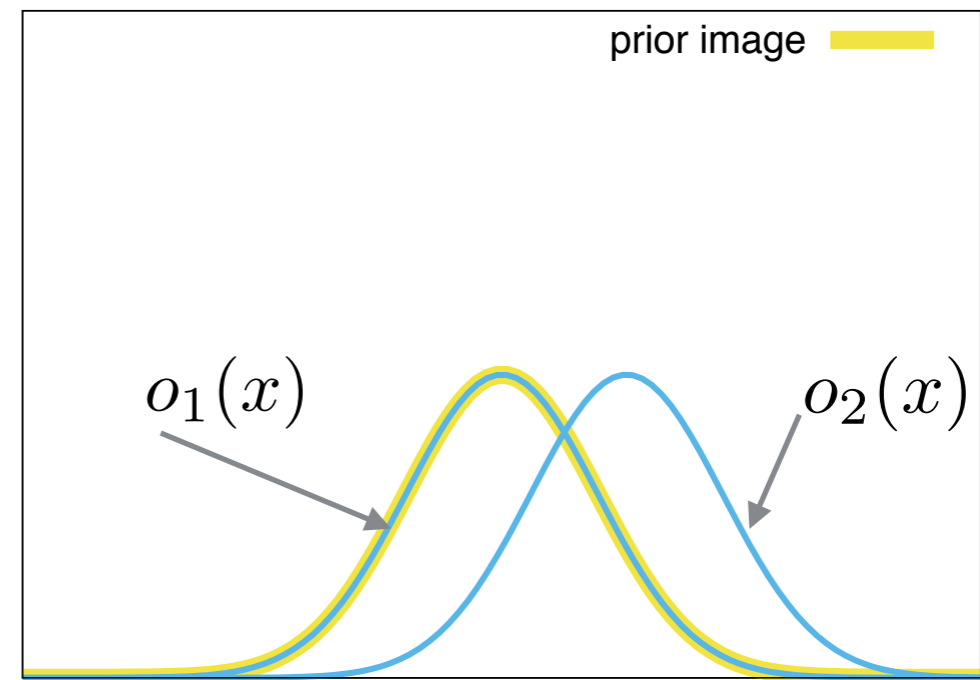
$o_k(\mathbf{x})$: images normalised to $\int o_k(\mathbf{x}) d\mathbf{x} = 1$

2. Example: assuming a Gaussian prior normalized to integral 1: Minimum of $H[o_k(\mathbf{x})]$



$$H[o_1(x)] < H[o_2(x)]$$

$$H[o_1(x)] < H[o_3(x)]$$



$$H[o_1(x)] < H[o_2(x)]$$

➔ absolute minimum of the regularisation function if $o_k(x) = prior(x)$!
the regularisation function tries to draw the images to the shape and position of the prior

Regularization - regularization functions

2. „Maximum entropy“ enforcing smoothness

$$H[o_k(\mathbf{x})] := \int \left\{ o_k(\mathbf{x}) \cdot \log \left\{ \frac{o_k(\mathbf{x})}{\text{prior}(\mathbf{x})} \right\} - o_k(\mathbf{x}) + \text{prior}(\mathbf{x}) \right\} d\mathbf{x}$$

3. „Pixel difference“ quadratic regularisation function

$$H[o_k(\mathbf{x})] := \int \frac{[|o_k(\mathbf{x}) - o_k(\mathbf{x} + \Delta\mathbf{x})|^2 + |o_k(\mathbf{x}) - o_k(\mathbf{x} + \Delta\mathbf{y})|^2]}{\text{prior}(\mathbf{x})} d\mathbf{x}$$

this function enforces smoothness, since it has its minimum value for very small pixel intensity differences

4. „Edge preserving & smoothness“ :

$$H[o_k(\mathbf{x})] := \int \frac{[\sqrt{|o_k(\mathbf{x}) - o_k(\mathbf{x} + \Delta\mathbf{x})|^2 + |o_k(\mathbf{x}) - o_k(\mathbf{x} + \Delta\mathbf{y})|^2 + \epsilon^2} - \epsilon]}{\text{prior}(\mathbf{x})} d\mathbf{x}$$

if $\epsilon^2 \gg [|o_k(\mathbf{x}) - o_k(\mathbf{x} + \Delta\mathbf{x})|^2 + |o_k(\mathbf{x}) - o_k(\mathbf{x} + \Delta\mathbf{y})|^2]$, i.e. small pixel intensity differences = smooth areas, $\longrightarrow H[o_k(\mathbf{x})]$ is nearly identical to the „pixel difference“ quadratic function enforcing smoothness.

In the other case, it is identical to the total variation regularisation function preserving important details, such as edges (Rudin et al. 1992).

Minimization algorithms to find the reconstructed image

- in many image reconstruction algorithms, the minimisation of the cost function $J[o_k(\mathbf{x})]$ is performed by **large-scale, bound-constrained nonlinear** optimisation algorithms using the gradient of the cost function to find the solution
- **large-scale** : because of the **huge number of image pixels** in the reconstruction;
 $o_k(\mathbf{x})$ is considered as a **NxN dimensional vector with the pixel intensities as coordinate values** (NxN number of pixel of the reconstruction)
- **bound-constrained**: because of the **positivity of the pixel intensities** = coordinate values
→ coordinate values >0
- **nonlinear**: because of the **non-linearity of the cost function** (bispectrum & power spectrum)
- nearly all these optimization algorithms search for the position of the local minimum close by; this means that the start image should already be close/similar to the true image.

Only the image reconstruction algorithm MACIM, and may be another one, uses global minimum search (MACIM applies simulated annealing).

Minimization algorithms to find the reconstructed image

- a rough explanation of such a gradient based optimization algorithm for a 2D parameter space:

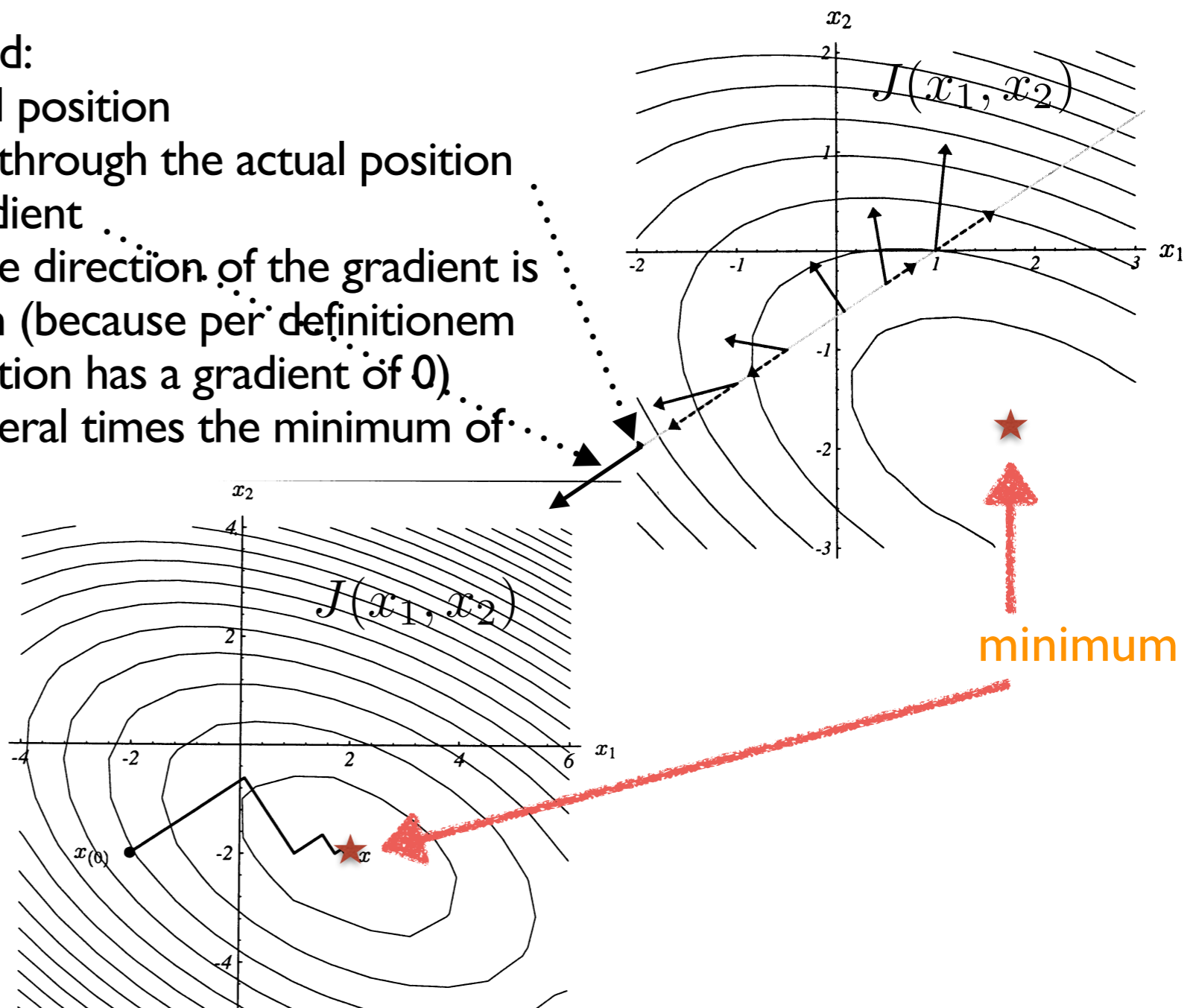
$$\text{gradient of the function } J(x_1, x_2) = \text{grad}\{ J(x_1, x_2) \} = \left(\frac{\partial J}{\partial x_1}, \frac{\partial J}{\partial x_2} \right)$$

is a 2D vector pointing always into the direction of the steepest increase of $J(x_1, x_2)$

Steps of the **Steepest Descent** method:

1. calculate the gradient of J at actual position
2. search for the minimum on a line through the actual position and along the direction of the gradient
3. at the position of the minimum the direction of the gradient is perpendicular to the line of search (because per definitionem the gradient at the minimum position has a gradient of 0)
4. after repeating steps 2) and 3) several times the minimum of $J(x_1, x_2)$ is reached.

contours showing the curves with the same value of J



Minimization algorithms to find the reconstructed image

- IRBis uses the nonlinear optimization algorithm ASA_CG (Hager & Zhang 2006);
ASA_CG is a conjugate gradient based large-scale, bound-constrained, nonlinear optimization algorithm

- Input to ASA_CG are

1. the actual position vector $(o_k(\mathbf{x}_1), o_k(\mathbf{x}_2), \dots, o_k(\mathbf{x}_j), \dots, o_k(\mathbf{x}_M))$

2. the value of the cost function $J[o_k(\mathbf{x}_1), o_k(\mathbf{x}_2), \dots, o_k(\mathbf{x}_j), \dots, o_k(\mathbf{x}_M)]$

3. the gradient of the cost function at the actual position vector

$$\text{grad}[J] = \left(\frac{\partial J[o_k(\mathbf{x})]}{\partial o_k(\mathbf{x}_1)}, \dots, \frac{\partial J[o_k(\mathbf{x})]}{\partial o_k(\mathbf{x}_j)}, \dots, \frac{\partial J[o_k(\mathbf{x})]}{\partial o_k(\mathbf{x}_M)} \right)$$

With these inputs ASA_CG works roughly similar as the „steepest descent method“ for searching the position of the local minimum.

Algorithm stops if the length of the gradient of the cost function is close to zero — if it is smaller than a given positive number.

Minimization algorithms to find the reconstructed image

- the gradient of the cost function is

$$\frac{\partial J[o_k(\mathbf{x})]}{\partial o_k(\mathbf{x}_j)} = \frac{\partial Q[o_k(\mathbf{x})]}{\partial o_k(\mathbf{x}_j)} + \mu \cdot \frac{\partial H[o_k(\mathbf{x})]}{\partial o_k(\mathbf{x}_j)}$$

with

$$\frac{\partial Q[o_k(\mathbf{x})]}{\partial o_k(\mathbf{x}_j)} = \int_{\mathbf{f}_u, \mathbf{f}_v \in M} 6 \cdot \frac{w_d(\mathbf{f}_u, \mathbf{f}_v)}{\sigma^2(\mathbf{f}_u, \mathbf{f}_v)} \cdot [\gamma_0 O_k^{(3)}(\mathbf{f}_u, \mathbf{f}_v) - O^{(3)}(\mathbf{f}_u, \mathbf{f}_v)]^* \times \\ \times O_k(\mathbf{f}_u) O_k(\mathbf{f}_v) \cdot \exp [+2\pi i (\mathbf{f}_u + \mathbf{f}_v) \cdot \mathbf{x}_j] d\mathbf{f}_u d\mathbf{f}_v$$

Scan of image reconstruction parameter in IRBis

- main reconstruction parameters are:

1. size of the binary circular mask in image space:

only within the mask, reconstructed intensities >0 are allowed;

the mask enforces the algorithm to reconstruct images with smoother Fourier spectra

(because small structures in image plane produce large, smooth structures in Fourier plane)

2. strength of the regularization parameter μ :

balancing the influence of the measured data (χ^2 term) and the prior data (regularization term) to the reconstruction: high μ value = strong influence of the prior term

- to find a good reconstruction these 2 parameters are varied:

outer loop: n (~ 6) different mask radii (usually mask radii increase within this loop*)

inner loop: m (~ 6) different values of the regularisation parameter;

for each image mask, m reconstruction runs with m μ values are performed (usually, the μ values decrease from one to the next run*)

* increasing mask radii / decreasing μ values:

stronger regularization at the beginning helps to come closer to the

absolute minimum of the cost function $J[O_k(\mathbf{x})]$ and helps to find the correct image

Scan of image reconstruction parameter in IRBis

- the $n \times m$ reconstructions obtained will be evaluated roughly according to their quality and sorted according to decreasing quality (the best reconstruction and a few of the next best reconstructions will be stored)
- the image quality is evaluated with a quality measure „ Q_{rec} " discussed on the next slide
- start & prior for the first run are the images defined at the beginning of the reconstruction session: a model image, e.g. a Gaussian, Uniform disk or a more physical model.

start & prior image for the actual run are the reconstruction of the run before:
this was found out to be a good choice and this is the default setting in IRBis

- the next image mask radius is obtained by adding a radius step to the actual radius:

$$R(j + 1) = R(j) + \Delta R$$

- the next regularisation parameter μ is obtained by multiplying the actual μ by a factor:

$$\mu(j + 1) = \mu(j) \cdot \text{factor}$$

Quality criterion of the reconstructions in IRBis

- the quality of the reconstruction can be evaluated by its χ^2 values:

a) reduced χ^2 of the squared visibilities :
$$\chi_{V^2}^2 = \frac{1}{N_{V^2}} \int_{\mathbf{f} \in \mathbf{M}} \left| \frac{V_k^2(\mathbf{f}) - V^2(\mathbf{f})}{\sigma_{V^2}(\mathbf{f})} \right|^2 d\mathbf{f}$$

b) reduced χ^2 of the closure phases :
$$\chi_{CP}^2 = \frac{1}{N_{CP}} \int_{\mathbf{f}_u, \mathbf{f}_v \in \mathbf{M}} \left| \frac{\beta_k(\mathbf{f}_u, \mathbf{f}_v) - \beta(\mathbf{f}_u, \mathbf{f}_v)}{\sigma_{\beta}(\mathbf{f}_u, \mathbf{f}_v)} \right|^2 d\mathbf{f}_u d\mathbf{f}_v$$

N_{V^2}, N_{CP} : number of measured elements

Good fit to the data : reduced $\chi^2 \approx 1$, because the deviations between measured and fitted data lies within the error bars.

Quality criterion of the reconstructions in IRBis

- Additional measure of the reconstruction quality is the so called residual ratio:

a) residual ratio of the squared visibilities :

$$\rho\rho_{V^2} := \frac{\int_{\mathbf{f} \in M_+} [V_k^2(\mathbf{f}) - V^2(\mathbf{f})] / \sigma_{V^2(\mathbf{f})} d\mathbf{f}}{\int_{\mathbf{f} \in M_-} [V_k^2(\mathbf{f}) - V^2(\mathbf{f})] / \sigma_{V^2(\mathbf{f})} d\mathbf{f}}$$

b) residual ratio of the closure phases :

$$\rho\rho_{CP} := \frac{\int_{\mathbf{f}_u, \mathbf{f}_v \in M_+} [\beta_k(\mathbf{f}_u, \mathbf{f}_v) - \beta(\mathbf{f}_u, \mathbf{f}_v)] / \sigma_{\beta(\mathbf{f}_u, \mathbf{f}_v)} d\mathbf{f}_u d\mathbf{f}_v}{\int_{\mathbf{f}_u, \mathbf{f}_v \in M_-} [\beta_k(\mathbf{f}_u, \mathbf{f}_v) - \beta(\mathbf{f}_u, \mathbf{f}_v)] / \sigma_{\beta(\mathbf{f}_u, \mathbf{f}_v)} d\mathbf{f}_u d\mathbf{f}_v}$$

M_+, M_- define the elements with positive and negative residuals, respectively

Good fit to the data : $\rho\rho \approx 1$ because in this case the fit is balanced between negative and positive residuals

- A global measure of the reconstruction quality

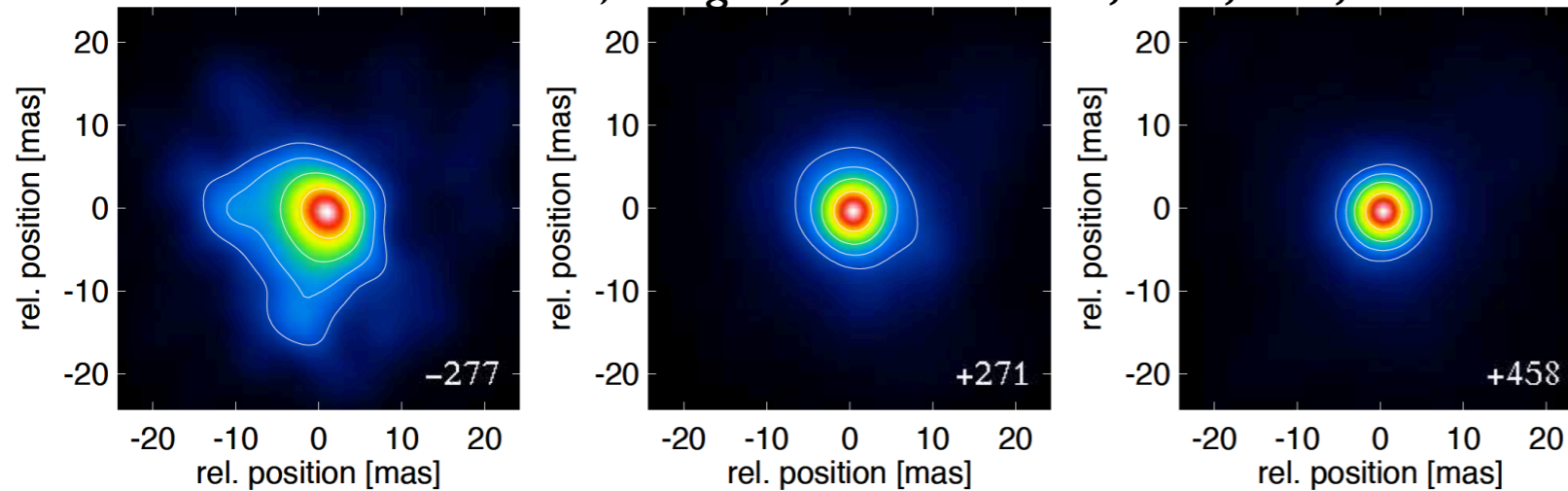
→ $Q_{\text{rec}} := 1/4 \cdot [|\chi_{V^2}^2 - 1| + |\rho\rho_{V^2} - 1| + |\chi_{CP}^2 - 1| + |\rho\rho_{CP} - 1|]$

Good reconstruction with Q_{rec} close to zero.

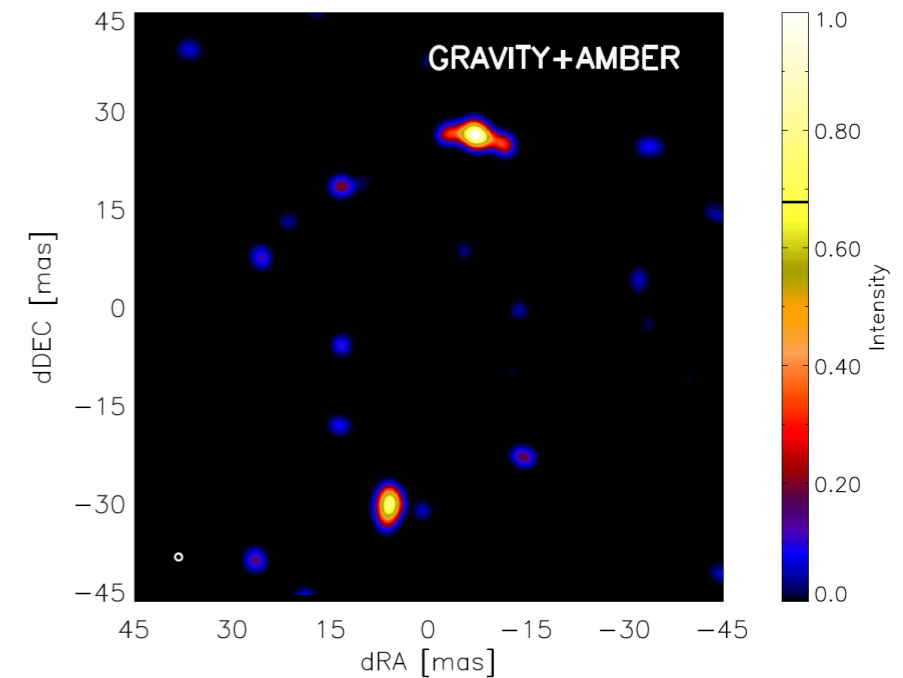
IRBis has been applied to several projects:

Hofmann, K.-H., Weigelt, G., Schertl, D. 2014, A&A, 565, A48

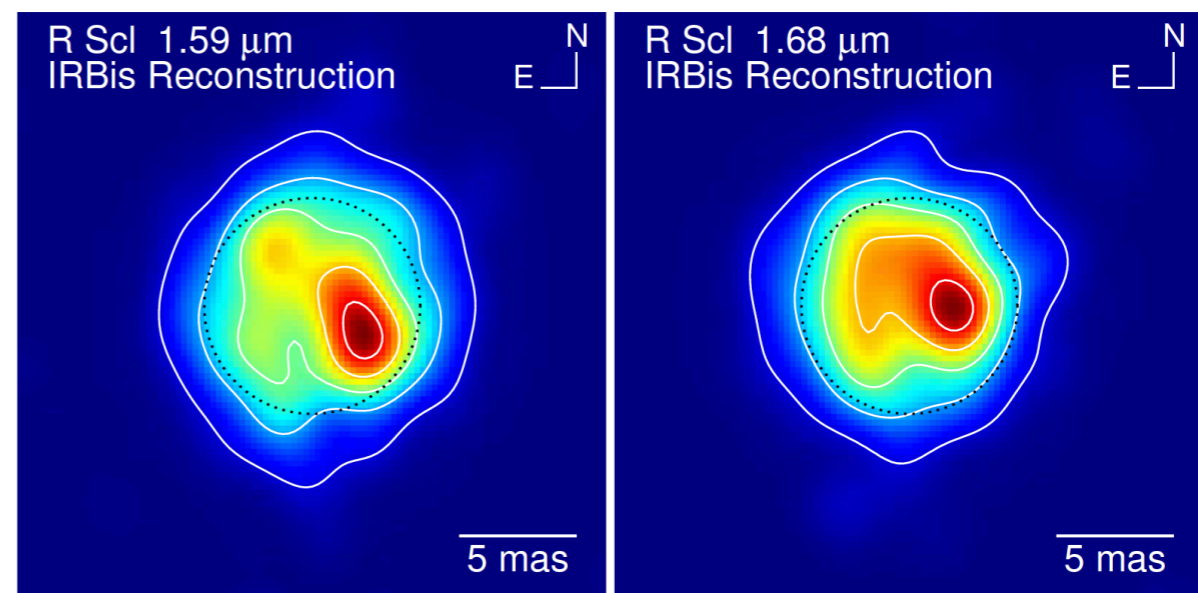
- „VLT-AMBER velocity-resolved aperture-synthesis imaging of η Carinae with a spectral resolution of 12000“, *Weigelt, G. et al. 2016, A&A, 594, A106*



- „A High-mass Protobinary System with Spatially Resolved Circumstellar Accretion Disks and Circumbinary Disk“, *Kraus, S. et al. 2017, ApJ, 835, L5*



- „Aperture synthesis imaging of the carbon AGB star R Sculptoris“, *Wittkowski, M., et al. 2017, A&A, accepted*



Other image reconstruction algorithms (chronological order)

- **BBM** (Building Block Method)

authors: Hofmann, Weigelt

optimization: direct optimization, using the gradient of the cost function in a simple way

regularization: with and without MEM

publications: Hofmann, K.-H. & Weigelt, G. 1993: *in Astronomy & Astrophysics 278(1)*, 328

Hofmann, K.-H. & Weigelt, G. 1991: *in F. Merkle (ed.), High Resolution Imaging by Interferometry II, ESO*

- **BSMEM** (BiSpectrum Maximum Entropy Method)

authors: Buscher, Baron, Young

optimization: Non-linear conjugate gradient method (MEMSYS library)

regularization: one regularization function: MEM-prior

publications: Buscher, D. 1994: *in J.G. Robertson, W.T. Tango (eds.), 158. IAU Symposium, 11-15 January 1993, p.91*

Young, J. 2004 (*Beauty Contest 2004*): *in W. Traub (ed.), Frontiers in Stellar Interferometry, Vol. 5491, pp. 886-899, SPIE*

- **MIRA** (Multi-aperture Image Reconstruction Algorithm)

authors: Thiebaut

optimization: VMLM-B (quasi-Newton method with bounds on the parameters)

regularization: many regularisation functions

publications: Thiebaut, E. 2002: *in J.-L. Starck, F.D. Murtagh (eds.), Astronomical Data Analysis II, Vol. 4847, pp. 174-183, SPIE*

Thiebaut, E. 2004: (*Beauty Contest 2004*): *in W. Traub (ed.), Frontiers in Stellar Interferometry Vol. 5491, pp. 886-899, SPIE*

Other image reconstruction algorithms

- **WISARD** (Weak-phase Interferometric Sample Alternating Reconstruction Device)
 - authors: Meimon, Mugnier, le Besnerais
 - optimization: VMLM-B plus a self-calibration step (to get Fourier phases out of the CPs)
 - regularization: many regularization functions
 - publications: Meimon, S., Mugnier, L.M., le Besnerais, G. 2004 (*Beauty Contest 2004*): in W.Traub (ed.), *Frontiers in Stellar Interferometry*, Vol. 5491, pp. 886-899, SPIE
 - Meimon, S., Mugnier, L.M., le Besnerais, G. 2005: *Optics Letters* 30(14), 1809

- **MACIM** (MArkov Chain IMager)
 - authors: Ireland, Monnier
 - optimization: global optimization with simulated annealing
 - regularization: MEM
 - publications: Ireland, M., Monnier, J. & Thureau, N. 2006: in J.D. Monnier, M. Schoeller, W. Danchi (eds.), *Advances in Stellar Interferometry*, Vol. 6268, pp. 6268 I T-1, SPIE

- **SQUEEZE**
 - authors: Baron, Monnier, Kloppenborg
 - optimization: based on MACIM; parallel tempering
 - regularization: MEM
 - publications: Kloppenborg, B. & Monnier, J., 2010 (*Beauty Contest 2010*): in W. Danchi, F. Delplancke, J.K., Rajagopal (eds.), *Advances in Stellar Interferometry*, Vol. 7734, pp. 77342N-1, SPIE

Other image reconstruction algorithms

Differences between the algorithms

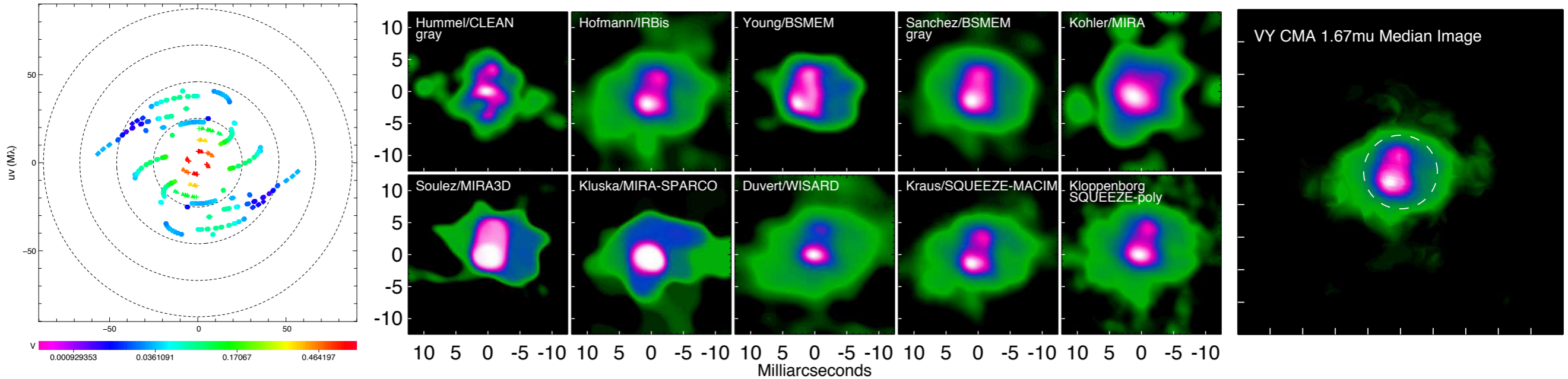
- Treatment of the observables
 - direct use of the observable (squared visibilities, closure phases) e.g. in MIRA, BSMEM
 - forming the complex object bispectrum and its error bars from the observables, e.g. IRBis
 - explicit solving for Fourier phases (WISARD)
- Global of gradient optimization
 - Gradient optimization, e.g. in MIRA, BSMEM, IRBis
 - Global optimization, e.g. in MACIM, SQUEEZE
- Available regularisers

Other image reconstruction algorithms

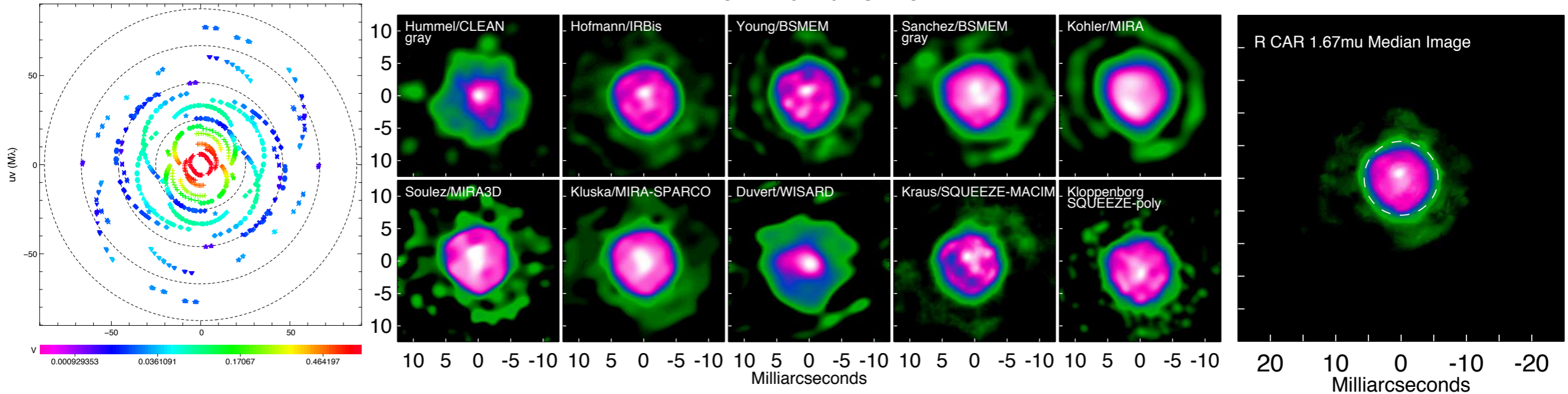
Imaging Beauty Contest 2014 - with real data from VLTI-PIONIER

- Observations of VY CMA and R Car with VLTI-PIONIER

VY CMA 1.67 μ FOV 25



R CAR 1.67 μ FOV 25



- all algorithms show more or less the same morphology
- median image is the average over all reconstructions showing the reliable structures

Enough data for image reconstruction?

- The number of independent uv points \geq the number of filled resolution elements = number of resolution elements within the image extent; use more than ~ 20 uv points!
- Holes in the uv coverage will give artefacts in the reconstructed image
- Shortest baseline B_{\min} should be well inside the first lobe of the target visibility (visibility ~ 0.5):

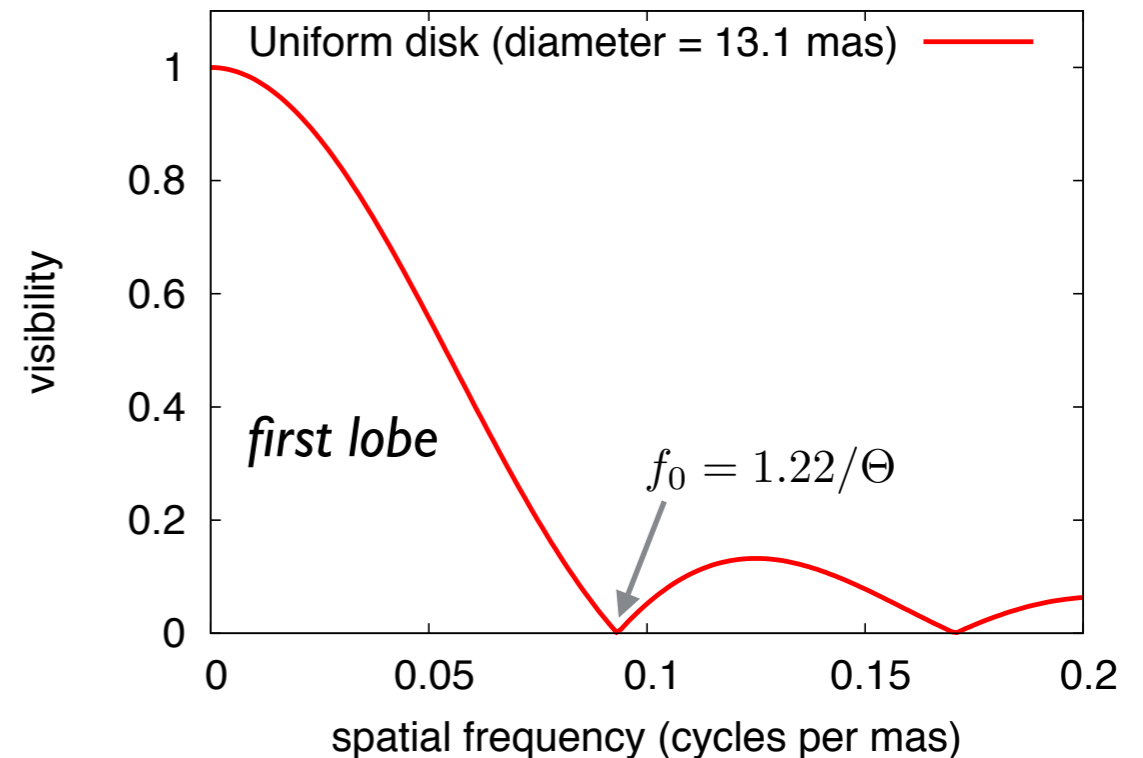
Example:

- a stellar disk is roughly a uniform disk (UD)
- the first zero of the visibility of a UD with angular diameter Θ lies at spatial frequency $f_0 = 1.22/\Theta$
- to get visibilities within the first lobe, i.e.

$$f < f_0 \longrightarrow \frac{B_{\min}}{\lambda} < \frac{1.22}{\Theta}$$

$$\longrightarrow \Theta < 1.22 \cdot \frac{\lambda}{B_{\min}} \approx \frac{1.22}{2} \cdot \frac{\lambda}{B_{\min}} =: \Theta_{\max}$$

due to the smallest baseline B_{\min} of the array: the diameter of the target should be not larger than Θ_{\max} .



Enough data for image reconstruction?

- Number of closure phases of a N-telescope interferometer = $\frac{N(N-1)(N-2)}{3 \cdot 2}$
 - Number of independent closure phases = $\frac{(N-1)(N-2)}{2}$
 - Number of phases (i.e. number of baselines) = $\frac{N(N-1)}{2}$
- number of independent closure phases < number of phases

Example N=4:

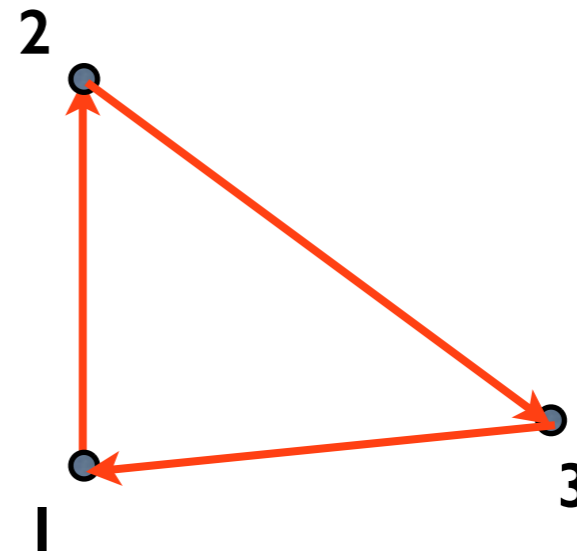
$$\Phi_{123} := \Phi_{124} + \Phi_{234} + \Phi_{314}$$

$$\Phi_{123} := \Phi_{12} + \Phi_{23} + \Phi_{31}$$

is a linear combination of 3 CPs;

because of $\Phi_{21} = -\Phi_{12}$ (real image)

$\Phi_{41} \& \Phi_{14}$ $\Phi_{24} \& \Phi_{42}$ $\Phi_{43} \& \Phi_{34}$ cancel! → Φ_{123}



Enough data for image reconstruction?

- Number of closure phases of a N-telescope interferometer = $\frac{N(N-1)(N-2)}{3 \cdot 2}$
 - Number of independent closure phases = $\frac{(N-1)(N-2)}{2}$
 - Number of phases (i.e. number of baselines) = $\frac{N(N-1)}{2}$
- number of independent closure phases < number of phases

Example N=4:

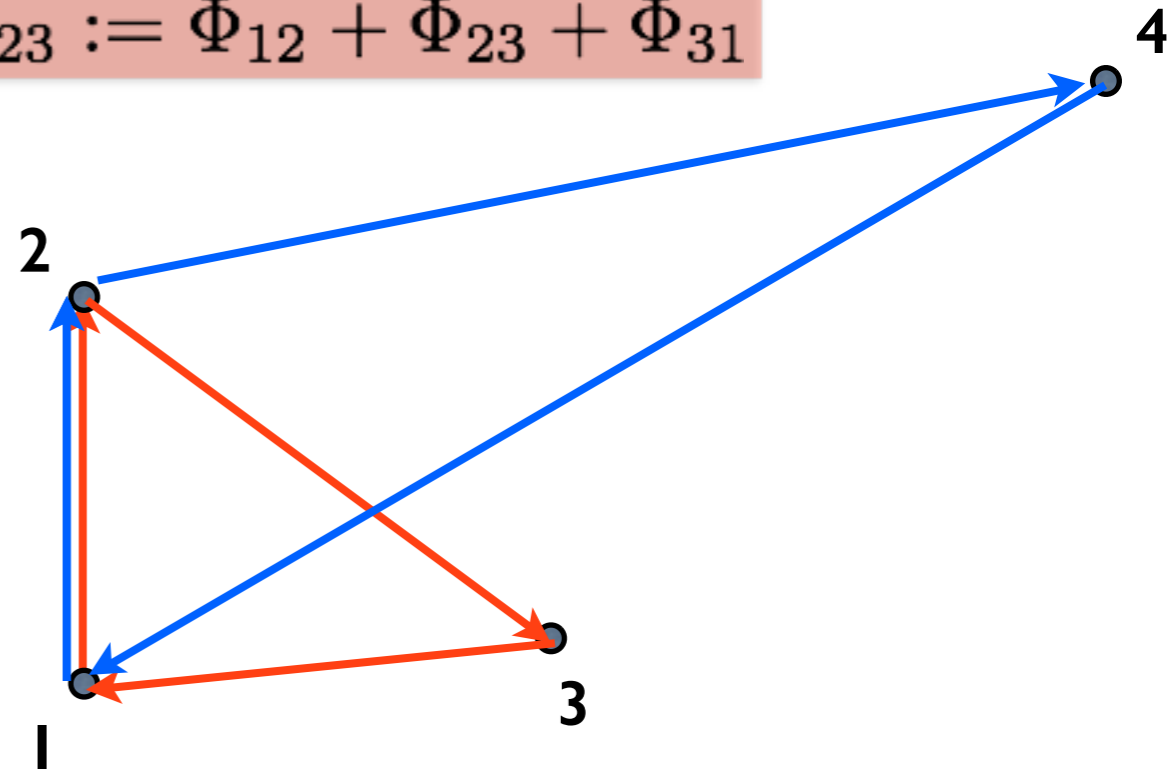
$$\Phi_{123} := \Phi_{124} + \Phi_{234} + \Phi_{314}$$

$$\Phi_{123} := \Phi_{12} + \Phi_{23} + \Phi_{31}$$

is a linear combination of 3 CPs;

because of $\Phi_{21} = -\Phi_{12}$ (real image)

$\Phi_{41} \& \Phi_{14}$ $\Phi_{24} \& \Phi_{42}$ $\Phi_{43} \& \Phi_{34}$ cancel! → Φ_{123}



Enough data for image reconstruction?

- Number of closure phases of a N-telescope interferometer = $\frac{N(N-1)(N-2)}{3 \cdot 2}$
 - Number of independent closure phases = $\frac{(N-1)(N-2)}{2}$
 - Number of phases (i.e. number of baselines) = $\frac{N(N-1)}{2}$
- number of independent closure phases < number of phases

Example N=4:

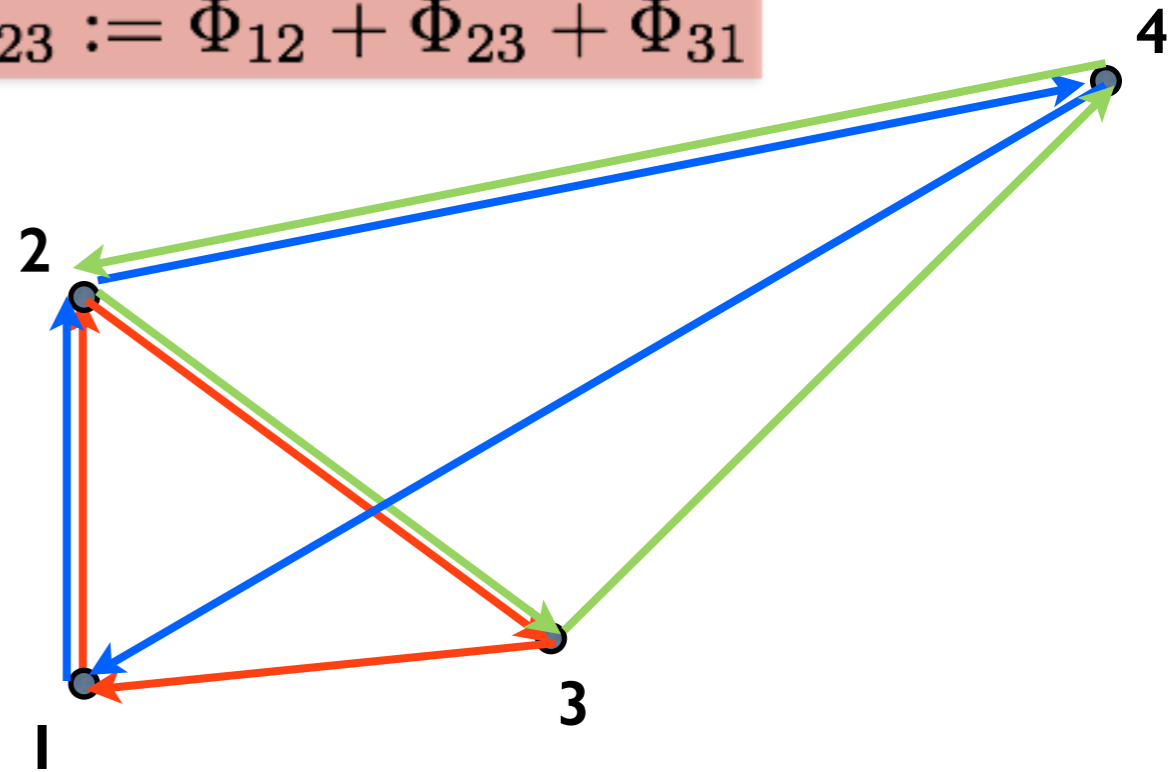
$$\Phi_{123} := \Phi_{124} + \Phi_{234} + \Phi_{314}$$

is a linear combination of 3 CPs;

because of $\Phi_{21} = -\Phi_{12}$ (real image)

$\Phi_{41} \& \Phi_{14}$ $\Phi_{24} \& \Phi_{42}$ $\Phi_{43} \& \Phi_{34}$ cancel! → Φ_{123}

$$\Phi_{123} := \Phi_{12} + \Phi_{23} + \Phi_{31}$$



Enough data for image reconstruction?

- Number of closure phases of a N-telescope interferometer = $\frac{N(N-1)(N-2)}{3 \cdot 2}$
 - Number of independent closure phases = $\frac{(N-1)(N-2)}{2}$
 - Number of phases (i.e. number of baselines) = $\frac{N(N-1)}{2}$
- number of independent closure phases < number of phases

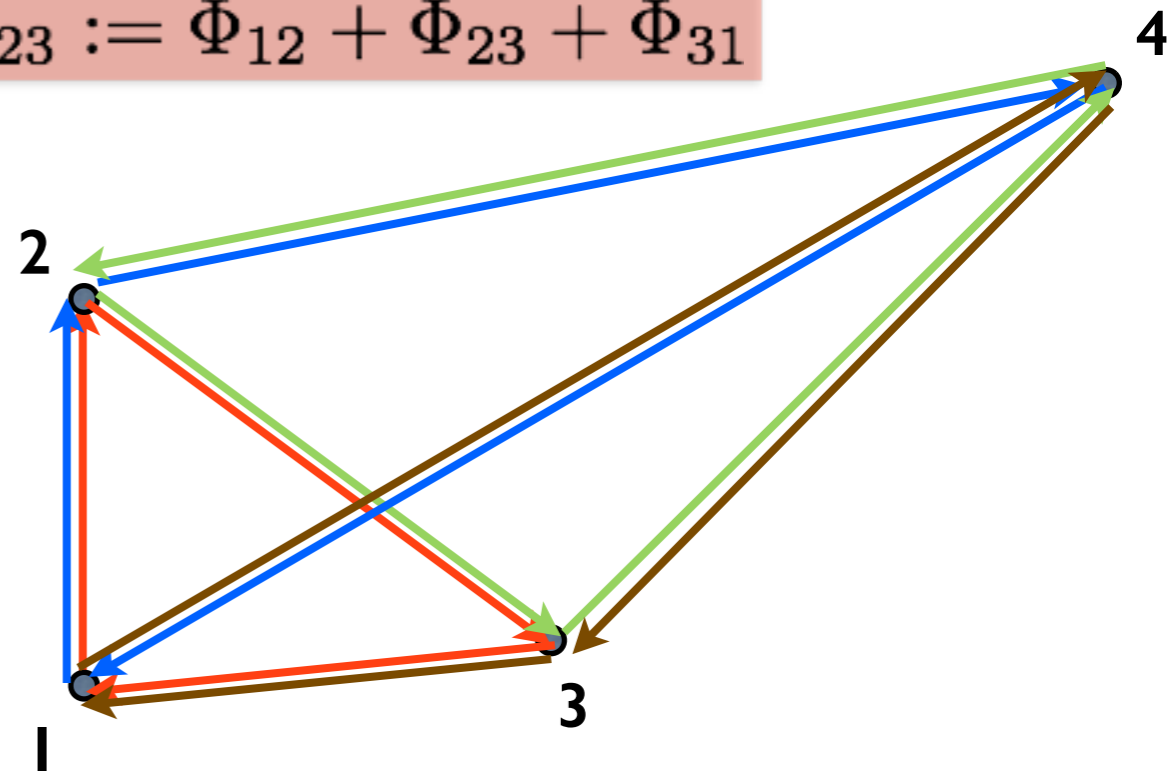
Example N=4:

$$\Phi_{123} := \Phi_{124} + \Phi_{234} + \Phi_{314}$$

$$\Phi_{123} := \Phi_{12} + \Phi_{23} + \Phi_{31}$$

is a linear combination of 3 CPs;
because of $\Phi_{21} = -\Phi_{12}$ (real image)

$\Phi_{41} \& \Phi_{14}$ $\Phi_{24} \& \Phi_{42}$ $\Phi_{43} \& \Phi_{34}$ cancel! → Φ_{123}



Enough data for image reconstruction?

- Number of closure phases of a N-telescope interferometer = $\frac{N(N-1)(N-2)}{3 \cdot 2}$
 - Number of independent closure phases = $\frac{(N-1)(N-2)}{2}$
 - Number of phases (i.e. number of baselines) = $\frac{N(N-1)}{2}$
- number of independent closure phases < number of phases

Example N=4:

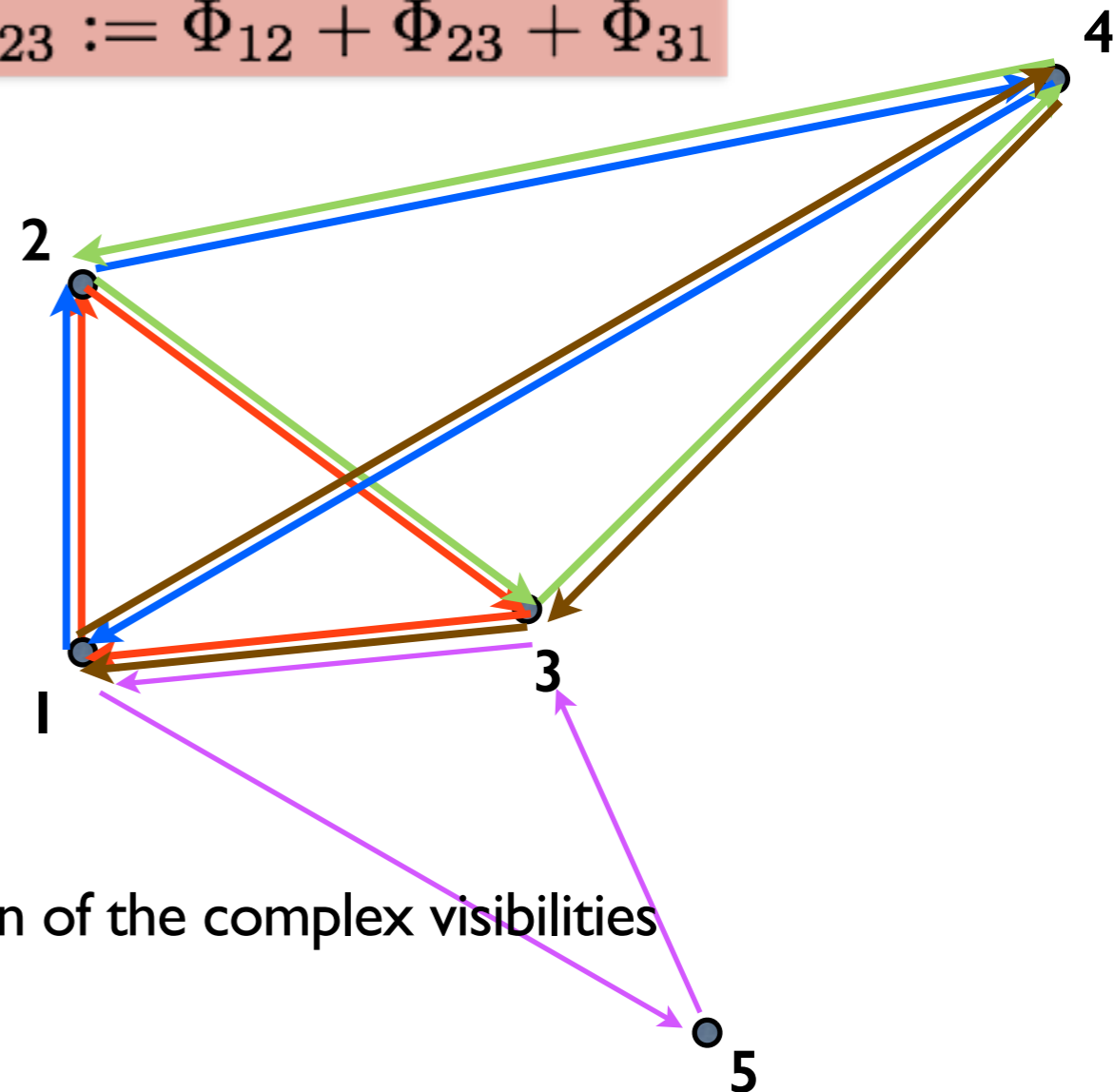
$$\Phi_{123} := \Phi_{124} + \Phi_{234} + \Phi_{314}$$

$$\Phi_{123} := \Phi_{12} + \Phi_{23} + \Phi_{31}$$

is a linear combination of 3 CPs;

because of $\Phi_{21} = -\Phi_{12}$ (real image)

$\Phi_{41} \& \Phi_{14}$ $\Phi_{24} \& \Phi_{42}$ $\Phi_{43} \& \Phi_{34}$ cancel! → Φ_{123}



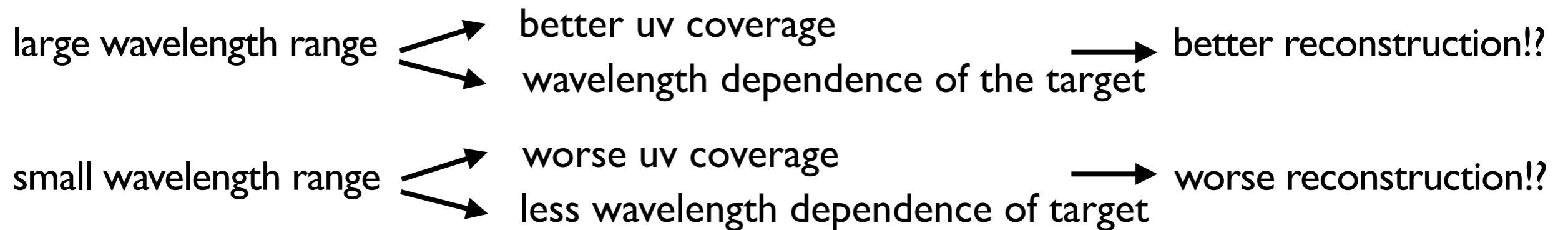
Example N=5:

In the same way,
each of the 4 CPs (in 1234) can be replaced
by the sum of 3 CPs including telescope 5
6 independent CPs

- 3 telescopes 1/3 of the Fourier phase information of the complex visibilities
- 4 telescopes 1/2
- 8 telescopes 3/4

Image reconstruction parameter

- **Wavelength range for image reconstruction:**



- Estimation of the **angular FOV** and the **number of pixels of the field to be reconstructed**
- **Size of the binary image mask**
- **Regularization function** and **regularization parameter μ**
- **Start image & prior image**

Image reconstruction parameter

- Estimation of the **angular FOV** and **number of pixels of the field to be reconstructed**

- to avoid cutting, the angular FOV should be $\sim 2-4x$ the size Θ of the target

- the highest spatial frequency in the Fourier plane of a $N \times N$ grid is $N/2$:
to avoid aliasing, all uv points should lie within a cut-off frequency at $\sim N/4$

with the relation $f_{\text{pixel}} = f \cdot FOV$, (valid for discrete Fourier transform)

the best value of N can be estimated by $\frac{N}{4} = \frac{B_{\text{max}}}{\lambda} \cdot FOV_{\text{max}}$

- **Size of the binary image mask** should be $> \Theta$ and could be $\leq FOV$ or larger

f : spatial frequency of a uv point in the data, for example,
 $B_{\text{max}}/\lambda =$ highest spatial frequency in the data

f_{pixel} : corresponding position vector in the Fourier plane of a $N \times N$ grid

FOV : angular FOV

Image reconstruction parameter

- **Regularization function** and **regularization parameter μ**
 - for extended and disk-like targets the „pixel difference“ quadratic regularisation function enforcing smoothness, the „edge preserving & smoothness“ regularization function, and maximum entropy yield good results
 - for binaries and other point-like objects the „pixel intensity“ quadratic regularization function is often successful
 - some regularization functions can be used with a prior image too, e.g. Gaussian, ...
 - regularization parameter μ controls the influence of the prior to the data penalty term
 - different start values of μ can be tested and the one that gives χ^2 values ~ 1 is selected
- **Start image & prior image** could be any geometrical model fitted to the measured data, e.g. Gaussian, Uniform disk, ...
or any more sophisticated physical model

Image reconstruction session with IRBis

- IRBis (= Image Reconstruction using the Bispectrum) is part of the contribution of the MPIfR Bonn to the ESO/VLTI beam combiner MATISSE built by an European consortium

IRBis is coded in C according to ESO standards and its technical name is „mat_cal_imarec“

the man page of IRBis can be called by: „esorex —man-page mat_cal_imarec“

the basic reconstruction run can be called by:

```
„esorex —log-dir=[directory of the logfile] —output-dir=[directory of the reconstruction results] \  
mat_cal_imarec [mat_cal_imarec options] [sof = ASCII file containing the input data]“
```

- for easier handling of an image reconstruction session with IRBis, a shell script, named „mat_cal_imarec.com“, is provided

Two actions of „mat_cal_imarec.com“:

1) Inspection of the data:

quality, wavelength range, baseline lengths,
a rough estimation of the size of the target by fitting a Gaussian, Uniform disk,
Fully darkened disk and a Lorentz function to the measured visibilities.

2) The reconstruction run with a presentation of the results.

Presentation of image reconstruction:

a) simulated data

b) PIONIER data

Image reconstruction session with IRBis

- I. action: estimation of some image reconstruction parameters

edit „mat_cal_imarec.com“:

- in „set data = “ insert the selected interferometric data (oifits format)
- switch on „I.action“ by setting „set guess = I“

after running of „mat_cal_imarec.com“ the calculated info is stored in „data.parameter“:

1. Information about the data:

- min./max. wavelength
- min./max. projected baseline length
- amount and quality of the data

2. Sizes of geometric models fitted to the squared visibilities ():

models: Gaussian, Uniform disk,

Note: for disk-like structures these sizes give the correct extension of the target, but, e.g. for binaries, these sizes represent not the target extension

3. Recommendations about the FOV and size of the NxN grid to be used for the reconstruction:

- max. meaningful target size : $\Theta_{\max} = \frac{1.22}{2} \cdot \frac{\lambda_{\max}}{B_{\min}}$
- FOV of the reconstruction : $FOV = 4 \times \Theta_{\max}$
- size of NxN grid with : $N = 4 \cdot \frac{B_{\max}}{\lambda_{\min}} \cdot FOV$

4. FOVs for different NxN grids with $N = 2^k$ are given:

the user can choose that NxN grid suitable for his target (FOV ~ 4 x target size)

Image reconstruction session with IRBis

- 2. action: image reconstruction run

edit „mat_cal_imarec.com“ by inserting:

- FOV of the reconstruction
- size of NxN pixel grid
- selected wavelength range

- Start radius of the binary circular image mask, the step size to create the next radius and the number of masks (~6 different radii):
$$\text{radius}(n) = \text{radius}(n-1) + \text{step size}$$
- Start value of the regularization parameter mu, the factor to create the next mu value and the number of mu values (~6 different values):
$$\text{mu}(m) = \text{mu}(m-1) * \text{factor}$$

- Number of Regularization function

- Power for the uv density weight:
 - each bispectrum element is weighted according to its position in the 4D uv plane
 - power = 0.5: uv density weight = inverse uv density with power of 0.5
 - power = 0 : uv density weight = 1 no weight!

- Select a start image and a prior image (prior image is used for regularization only):
 - could be read in (fits format), or
 - could be one of the 3 circular geometrical models produced in mat_cal_imarec:
Gaussian, Uniform disk, Fully darkened disk

Image reconstruction session with IRBis — Example

- Reconstruction of the Mira variable R Car observed with VLT/PIONIER instrument with 4 ATs (R Car was one target of the imaging beauty contest 2014)

- I.action: estimation of some image reconstruction parameter in ASCII file „data.parameter“

```
- minimum and maximum wavelength (in m)      : 1.66364e-06 1.68468e-06
- minimum and maximum baseline length (in m): 8.07256 133.912
- number of measured squared visibilities     : 902
- number of measured closure phases          : 465
- average SNR of measured squared visibilities: 24.4123
- average error of the closure phase (in deg) : 2.21985
```

--> recommended FOV of the reconstruction area:

```
- the size of target should be not larger than  $\Theta_{\max} = (1.22/2) \cdot \lambda_{\max} / B_{\min} = 26.258$  mas
- the optimal FOV[mas] should be at least  $4 \cdot \Theta_{\max} = 105.032$  mas
- the optimal FOV[mas] is covered by a  $N \times N$  pixel grid with  $N = 4 \cdot (B_{\max} / \lambda_{\min}) \cdot \Theta_{\max} = 163.952$ 
  (with this grid of size  $N$ , all uv points lie within the cut-off frequency  $f_{\text{pixel}} = N/4$  -> to avoid aliasing)
```

--> FOVs with the $f_{\text{pixel}} = N/4$ cut-off frequency for several $N \times N$ arrays:

```
* 16x16 pixels --> FOV = 10.25 mas
* 32x32 pixels --> FOV = 20.5 mas
* 64x64 pixels --> FOV = 41.0001 mas
* 128x128 pixels --> FOV = 82.0002 mas
* 256x256 pixels --> FOV = 164 mas
* 512x512 pixels --> FOV = 328.001 mas
```

Note: a) Choose that $N \times N$ pixel grid, where the FOV $\sim 4x$ the target size (e.g. derived from the geometrical model fits below).
b) If you take a smaller FOV for the $N \times N$ pixel grid as stated in the list above, this means that the uv point of the longest baseline is within $N/4$, which is no problem.

- Fits to the V^2 data:

```
* Gaussian --> FWHM = 7.599 mas (red.  $\chi^2 = 21.353$ ,)
* Uniform disk --> diameter = 10.220 mas (red.  $\chi^2 = 7463.333$ ,)
* Fully darkened disk --> diameter = 11.649 mas (red.  $\chi^2 = 342.480$ ,)
```

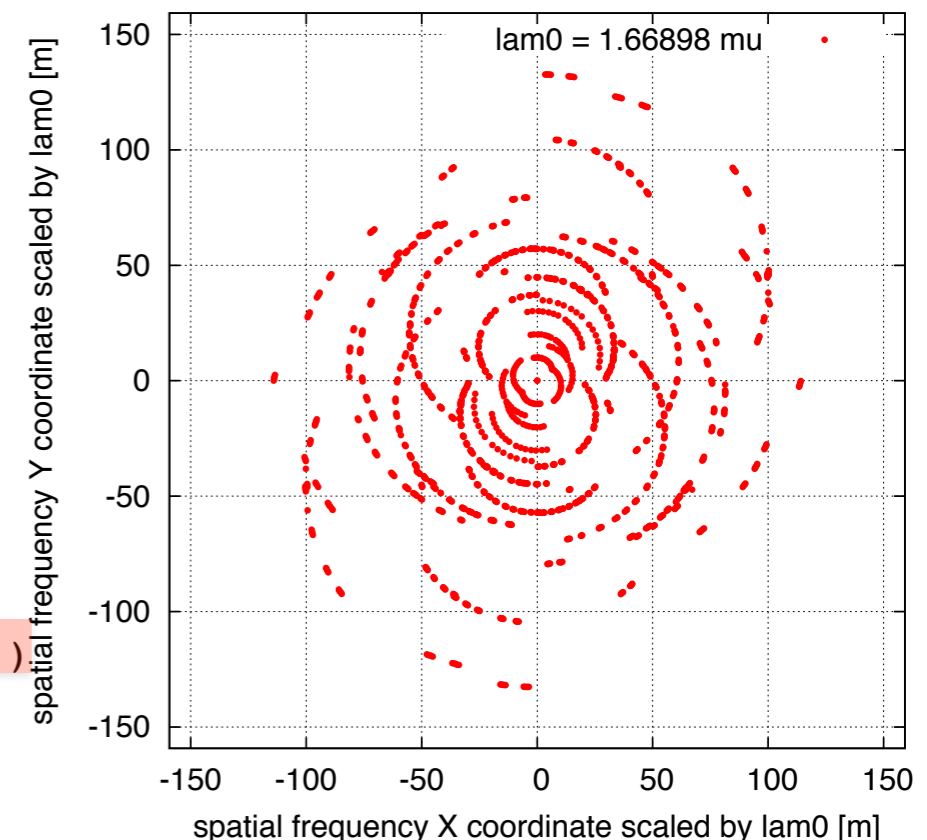


Image reconstruction session with IRBis — Example

- Reconstruction of the Mira variable R Car observed with VLT/PIONIER instrument (4 ATs)

- 2. action: image reconstruction run

start mode = 4: Fully Darkened Disk

```
# INPUT data
set objname = NameOfObject           # name of the target
set pfaad   = /home/user/Testcases/BeautyContest2014/Daten/ # absolute path to the interferometric data
set data    = ($pfaad/R_CAR_all.fits) # all interferometric data with oifits format with its path $pfaad/
set lambdaFrom = 1.66                # lambdaFrom - lambdaTo : wavelength intervall [mu]
set lambdaTo   = 1.69

# INPUT - parameter
set fov        = 60.0                # Field of view for the reconstructed image in [mas].
set npix       = 128                 # Size of the reconstructed image in pixels. Powers of 2 should be used (spee
set oradiusStart = 30.0 # 20.0        # start radius of the object mask [mas]
set stepSize    = 1.0                 # step size for the object mask radius scan [mas]; next radius = actual radiu
set oradiusNumber = 6                 # number of object mask radius scans
                                        # oradius(n) = oradiusStart + (n-1)*stepSize (n = 1..oradiusNumber)

set muStarts   = (0.1 0.01)          # start value(s) for the regularization parameter mu
set muFactor   = 0.5                  # next mu value is actual mu multiplied with mufactor
set muNumber   = 12                   # number of regularization parameter runs
                                        # mu(n) = muStart*muFactor^(n-1) (n = 1..muNumber)

set regFuncs   = (-4)                # regularisation function(s) (0 = no regularization)
                                        # = 1: pixel intensity quadratic: H(x,y) := Sum{|ok(x,y)|^2/prior(x,y)}
                                        # = 2: maximum entropy: H(x,y) := Sum{ok(x,y)*alog(ok(x,y)/prior(x
                                        # = 3: pixel difference quadratic: H(x,y) := Sum{[|ok(x,y)-ok(x+dx,y)|^2 + |o
                                        # = 4: edge preserving: H(x,y) := Sum{[sqrt[|ok(x+dx,y)-ok(x,y)|^2
                                        # = 5: smoothness: H(x,y) := Sum{|ok(x,y)-ok(x+dx,y+dy)|^2}/p
                                        # = 6: quadratic Tikhonov: H(x,y) := Sum{[|ok(x,y,z)-prior(x,y,z)|^2}
                                        # If a negative number (for example -4) is used, the prior image is set to a
set regEps     = 1.0                  # Epsilon for regularisation function 4 (edge preserving) only
set weightPower = 0.0                # power for the uv density weight

set startmode  = 4                    # 0 = read from file, 1 = point source, 2 = gaussian disc, 3 = uniform disc,
set startparam = 11.65                # startmode=0 -> scale [mas/px], mode=2 -> FWHM [mas], mode=3 -> diameter [ma

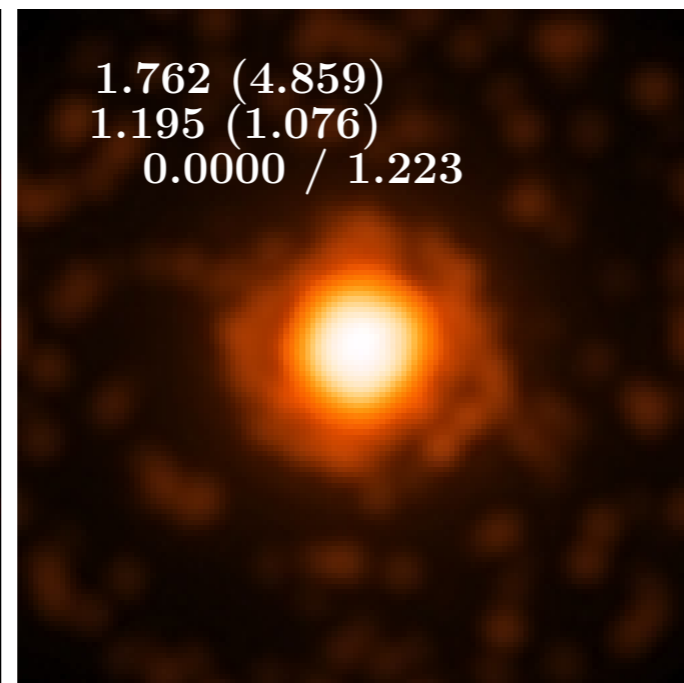
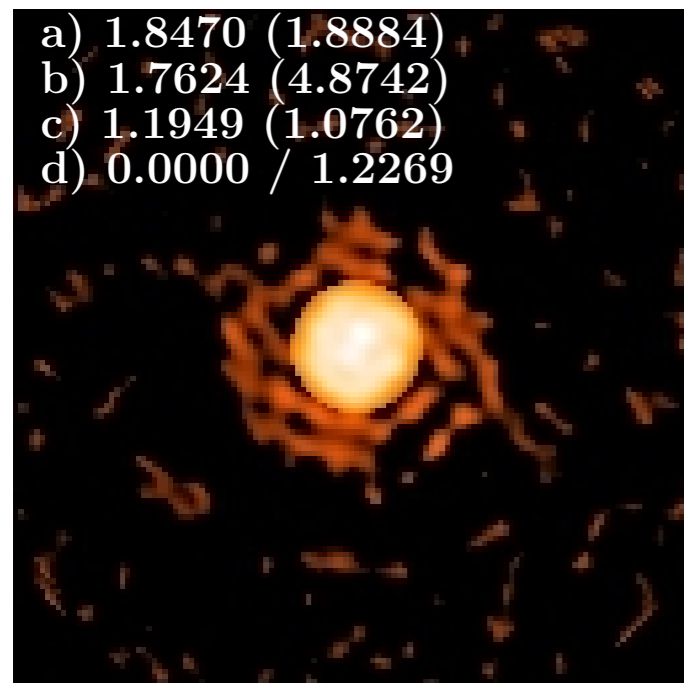
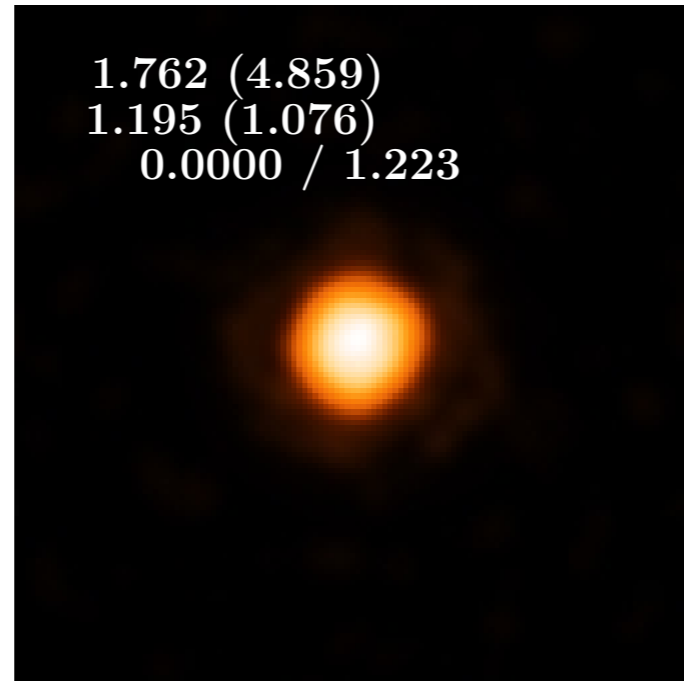
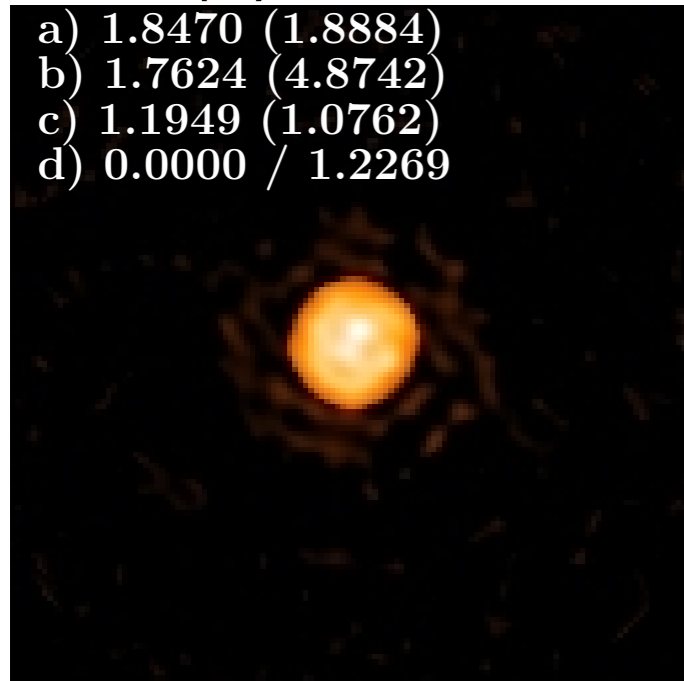
set priormode  = $startmode           # 0 = read from file, 1 = point source, 2 = gaussian disc, 3 = uniform disc,
set priorparam = $startparam          # mode=0 -> scale [mas/px], mode=2 -> FWHM [mas], mode=3 -> diameter [mas], m
```

Image reconstruction session with IRBis — Example

- Reconstruction of the Mira variable R Car observed with VLT/PIONIER instrument (4 ATs)

reconstruction parameter: FOV = 60mas, 64x64 grid, image mask radii 30-36mas

linear display

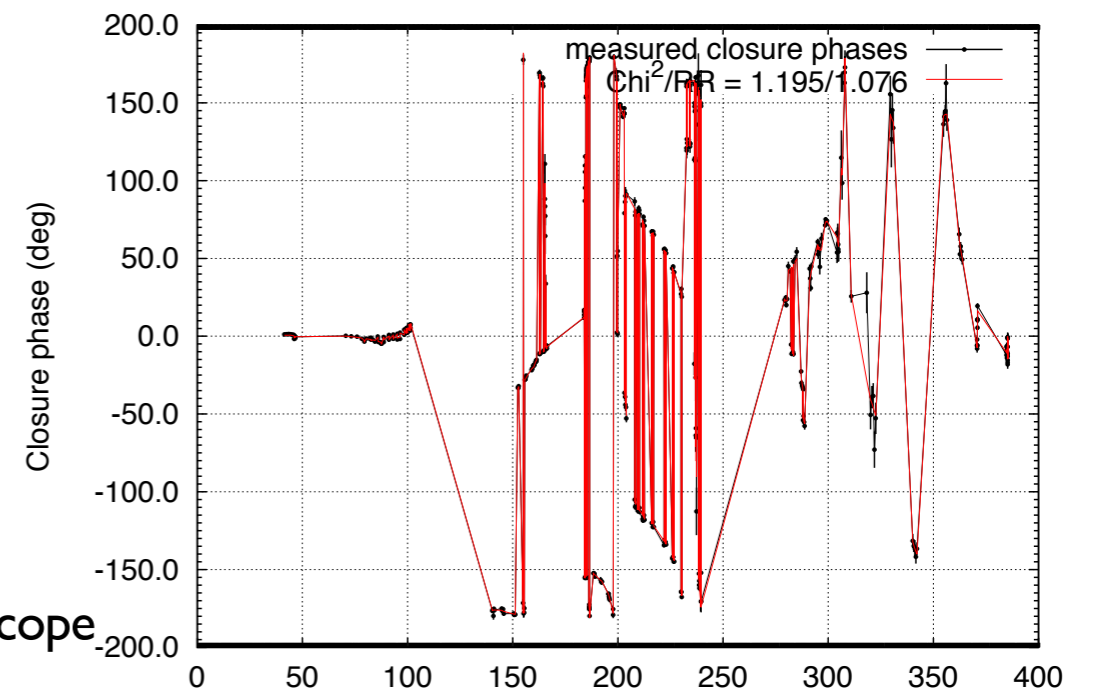
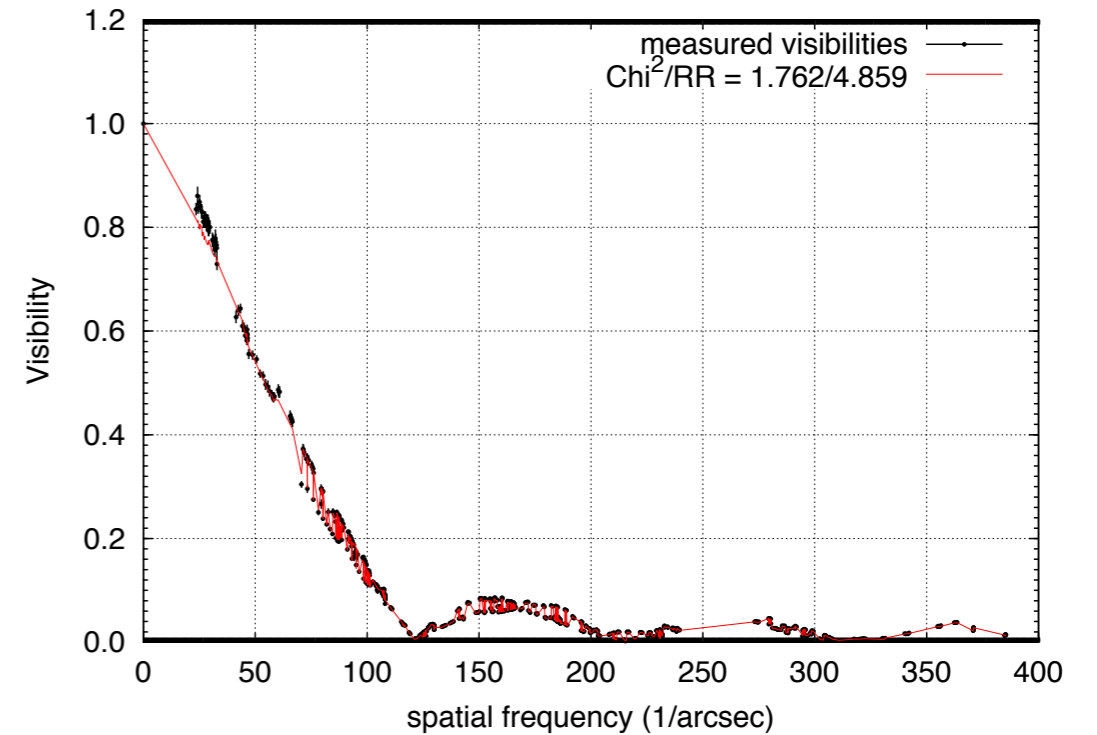


sqrt display

unconvolved

convolved with PSF of 133.9m telescope

(longest baseline = 133.9 m)



How to judge the quality of a reconstruction — what features are real?

Usually it is not possible to identify a „noise level“ in the reconstruction because of regularization and artefacts due to the sparse uv coverage.

Instead we have to consider:

- Are features robust against changing the reconstruction parameter?
- Are the χ^2 values and residual ratio values $\rho\rho$ close to 1?
- Compare reconstructions from independent subsets of the data
 - split by wavelength or by time
- Image reconstructions with simulated data of a model of the target, with the same uv coverage and the same SNR as the science data

How to improve the reconstruction?

- Adjust the size of the FOV to be reconstructed and the size of the corresponding NxN grid to the reconstructed object
- Use the reconstructed object as start and/or prior object
 - initial reconstruction can be smoothed or thresholded and then used as model for the next run
- Use different regularization functions and different regularization parameter
- Test with a larger or smaller binary mask size
- Test with a larger wavelength range
 - Trade between improved uv coverage and intrinsic variation of the object with wavelength

Summary and Outlook

- most of the present image reconstruction algorithms derive the image of the object directly from the measured bispectrum, or closure phases and visibilities; their task is:
 - „Find that image which has, within the error bars, the same bispectrum values as the measured bispectrum“
- they do that task by minimizing the χ^2 function with different optimization algorithms
- but because of the non-linearity of the data and the sparse uv coverage prior information and regularization has to be used to find the correct image of the target
- future: multi-spectral data image reconstruction
 - beam combiner, like AMBER, GRAVITY and MATISSE, provide simultaneous measurements in many spectral channels;
 - future image reconstruction algorithms will x-y- λ images using the fact that the targets have show smooth transition between neighbouring spectral channels.

